1991

Structures and thermodynamics of some rare earth sulfides

Yan Zhang
Iowa State University

INFORMATION TO USERS

This manuscript has been reproduced from the microfilm master. UMI films the text directly from the original or copy submitted. Thus, some thesis and dissertation copies are in typewriter face, while others may be from any type of computer printer.

The quality of this reproduction is dependent upon the quality of the copy submitted. Broken or indistinct print, colored or poor quality illustrations and photographs, print bleedthrough, substandard margins, and improper alignment can adversely affect reproduction.

In the unlikely event that the author did not send UMI a complete manuscript and there are missing pages, these will be noted. Also, if unauthorized copyright material had to be removed, a note will indicate the deletion.

Oversize materials (e.g., maps, drawings, charts) are reproduced by sectioning the original, beginning at the upper left-hand corner and continuing from left to right in equal sections with small overlaps. Each original is also photographed in one exposure and is included in reduced form at the back of the book.

Photographs included in the original manuscript have been reproduced xerographically in this copy. Higher quality 6" x 9" black and white photographic prints are available for any photographs or illustrations appearing in this copy for an additional charge. Contact UMI directly to order.

U·M·I

University Microfilms International
A Bell & Howell Information Company
300 North Zeeb Road, Ann Arbor, MI 48106-1346 USA
313/761-4700 800/521-0600

Order Number 9207258

Structures and thermodynamics of some rare earth sulfides

Zhang, Yan, Ph.D.

Iowa State University, 1991

U·M·I
300 N. Zeeb Rd.
Ann Arbor, MI 48106

Structures and thermodynamics of some rare earth sulfides

by

Yan Zhang

A Dissertation Submitted to the

Graduate Faculty in Partial Fulfillment of the

Requirements for the Degree of

DOCTOR OF PHILOSOPHY

Department: **Chemistry**
Major: **Physical Chemistry**

Approved:

Signature was redacted for privacy.

In Charge of Major Work

Signature was redacted for privacy.

For the Major Department

Signature was redacted for privacy.

For the Graduate College

Iowa State University
Ames, Iowa

1991

TABLE OF CONTENTS

GENERAL INTRODUCTION

The rare earth sulfides have been studied extensively due to the fact that they exhibit a wide variety of stoichiometries, structures and properties. Samsonov[1] reviewed their crystal structures, electron fine structures, thermal, magnetic, optical, chemical properties and preparation methods. In recent years, these materials have drawn increasing interest in their transport, optical, and magnetic properties.[2] Their high melting points and high stability to thermal shock make them valuable in manufacturing as high temperature crucibles and for other refractory uses. The rare earth monosulfides, except for EuS, SmS and YbS, are metallic conductors, while the sesquisulfides are often semiconducting or semimetallic in nature. Because the rare earth sulfides possess a variety of structures and properties, study of their thermodynamic properties will provide not only valuable information on the systematics of cohesive energies of materials, i.e., on the energetics of chemical bonding in nonmolecular solids, but also basic thermal data fundamental to the application of these compounds in modern high-temperature technology.

The existence of various regions of homogeneity for rare earth monosulfides has long been recognized.[1,3] Only in recent years has the phenomenon of vacancy ordering that occurs in some of these monosulfides when samples are slowly cooled down been

noticed. For example, scandium monosulfide has a homogeneity range from Sc/S = 0.806 to Sc/S = 1.14 with a NaCl type structure at high temperatures. Vacancy ordering in this compound is known to occur below 973 K[4,5] for the composition $Sc_{0.8}S$. The structure changes from cubic to rhombohedral with decreasing temperatures. Another example is ytterbium monosulfide, which has a region of homogeneity from $Yb_{0.878}S$ to $Yb_{0.9}S$ with the NaCl type structure at high temperatures. A recent study[6] showed that $Yb_{0.877}S$ has a superstructure of the NaCl-type structure at low temperatures. In order to understand the existence and stability of the ordered phases and the width of the homogeneity ranges of these nonstoichiometric solids, the thermodynamic properties of both the defect phases and their adjacent phases need to be investigated.

Studies of the chemical behavior of rare earth sulfide systems at high temperature depend fundamentally upon a knowledge of the condensed phases present in the systems at high temperatures. The methods used for many years to synthesize rare earth sulfides start from a mixture of the elements with the desired stoichiometry or from passing H_2S through rare earth oxide. To find all the existing phases in a composition range of interest by these methods is very tedious. In our high temperature vaporization studies, we can, using the Knudsen effusion method, nearly continuously monitor the phase changes as the composition changes by controlling the temperatures and

Knudsen cell orifice area. It occurs to us that the Knudsen effusion technique is a powerful and time-saving method to discover new phases and prepare known materials with precisely determined stoichiometry.

Due to ytterbium's stable electron configuration $4f^{14}5d^{0}6s^{2}$, ytterbium sulfide shows properties that differ from the other lanthanide sulfides except for Eu and Sm sulfides. For example, in their monosulfides, ytterbium, europium and samarium have only two valance electrons, and as a consequence these monosulfides are black semiconductors. On the other hand, the other lanthanide monosulfides, which have a 5d electron in the conduction band, are gold-colored, metallic conductors. A thermodynamic study[7] has shown that europium monosulfide behaves conspicuously differently from the other lanthanides. In this work, the investigation of the vaporization behavior and thermodynamics of Yb-S was undertaken to permit a comparison with the behavior of europium, and other lanthanide monosulfides, and thus contribute to the systematic understanding of the stability-electron structure relationship in the lanthanide sulfide series.

The vaporization and thermodynamic properties of the Nd-S system were investigated in this work for the following reasons: (1) The vaporization behavior of its neighboring systems Pr-S and Sm-S are different. Both PrS and Pr_3S_4 vaporize congruently in the Pr-S system[8] , while in the Sm-S system, Sm_3S_4 is the only congruent vaporizing composition. (2) The only standard enthalpy

of formation of $Nd_3S_4(s)$ was obtained by Finogenov's calorimetric study.[9] The details of the vaporization behavior and the partial pressures of the gaseous species have not been reported. The reported standard enthalpies of formation of $Nd_2S_3(s)$[8,10,11] are not in agreement.

The purpose of this work was to obtain information on the stoichiometry and structure of the neodymium sulfides, ytterbium sulfides and thulium sulfides, to find new compounds by the high-temperature Knudsen effusion method and to solve their structures by single crystal x-ray diffraction techniques, and to study the high temperature vaporization behavior of the Yb-S and Nd-S systems and thus to obtain the thermodynamic data for these systems.

Explanation of Dissertation Format

This dissertation presents results in three sections. Section one and two describe the high temperature vaporization behavior and thermodynamics of the Nd-S and Yb-S systems. Section three reports the structures of two new thulium sulfides: Tm_8S_{11} and $Tm_{15}S_{22}$, and the magnetic properties of Tm_8S_{11}. References cited in these sections are followed at the end of each individual section. The experimental techniques used for these three sections and the theory that the first and second sections are based on are described at the beginning of this

dissertation. References cited in general introduction, experimental and theory sections are collected at the end of this dissertation.

EXPERIMENTAL

Sample Preparation

The binary Nd-S, Yb-S and Tm-S compounds were prepared by reactions of mixed rare-earth metal sheets and sulfur. The Nd, Yb and Tm metal sheets (0.02" thick) were obtained from the Ames Laboratory materials preparation center with purities of 99.9%, 99.9% and 99.99% respectively. The chemical analyses of the bulk Nd, Yb and Tm are shown in Tables 1 - 3. The sulfur was obtained from Ventron with a purity of 99.9995%. The desired amount of rare-earth metal and sulfur with starting composition in the ranges S/M = 0.9 - 1.5 (M = Nd, Yb, Tm) was placed in a quartz ampoule which was previously outgassed using an oxygen-gas torch; the mixture of rare-earth metal and sulfur was introduced to the quartz ampoule in an argon atmosphere glove box. The reaction tube was evacuated to about 10^{-6} torr and sealed. The ampoule was heated in a tube furnace for several days until all the sulfur had been consumed. The temperature of the furnace was gradually raised from 400°C to 800°C in this period of time. The sample thus obtained was inhomogeneous with sulfur rich compounds coating the outside of unreacted metal strips. The sample was removed from the ampoule, pressed into a pellet, and then annealed in a tungsten container in vacuum (10^{-6} - 10^{-7} torr) using an induction furnace at high temperature (1300°C - 1700°C).

Table 1. Chemical analysis[a] of neodymium metal (Al code No. Nd -9181) by spark source mass spectrometer[b] and vacuum fusion[c]

Element	Atomic or Wt. (ppm)	Element	Atomic or Wt. (ppm)	Element	Atomic or Wt. (ppm)
Fe	10	Cl	4	Pt	<3
Ni	1	Cu	4	Ta	50
Nb	<2	Si	10	Cr	1
As	<500	Sc	6	Gd	2
La	3	Ce	2.8	Pr	1.2
O	522(58)[d]	N	175(17)	H	428(3)
C	96(8)	F	45(6)		

[a]Only these elements with atomic or Wt. ppm > 1 are listed.

[b]Elements from Fe to Pr were analyzed by spark source mass spectrometer (in atomic ppm).

[c]Elements from O to F were analyzed by vacuum fusion (in Wt. ppm).

[d]Uncertainties.

Table 2. Chemical analysis[a] of ytterbium metal (Al code No.Yb -72081) by spark source mass spectrometer[b] and vacuum fusion[c]

Element	Atomic or Wt. (ppm)	Element	Atomic or Wt. (ppm)	Element	Atomic or Wt. (ppm)
Li	4	Fe	4	Cl	200
Rb	<300	Na	<70	Ca	5
Sr	<300	W	1.8	Zn	5.3
Zr	1.3	Si	<70	Ce	1
Er	<2	O	<100(<10)[d]	N	<100(<10)
H	1713(10)	C	187(13)		

[a]Only these elements with atomic or Wt. ppm > 1 are listed.

[b]Elements from Li to Er were analyzed by spark source mass spectrometer (in atomic ppm).

[c]Elements from O to C were analyzed by vacuum fusion (in Wt. ppm).

[d]Uncertainties.

Table 3. Chemical analysis[a] of neodymium metal (Al code No. Tm -32387) by spark source mass spectrometer[b] and vacuum fusion[c]

Element	Atomic or Wt. (ppm)	Element	Atomic or Wt. (ppm)	Element	Atomic or Wt. (ppm)
Na	<6	Mg	2	Al	<40
Si	12	Cl	6.8	Ar	<4
K	10	Ca	4.5	Sc	<40
Cr	<2	Mn	<70	Fe	6.9
Cu	2	Ga	<30	Nb	<1
Mo	<2	Ru	<2	Pd	<2
Ag	<1	Cd	<2	Sn	<2
Te	<2	Xe	<2	Hf	<2
W	<2	Re	<2	Os	<2
Ir	<1	Pt	<2	Hg	<2
La	4.2	Nd	<2	Sm	<3
Eu	<2	Gd	<3	Dy	<3

Table 3. (continued)

Element	Atomic or Wt. (ppm)	Element	Atomic or Wt. (ppm)	Element	Atomic or Wt. (ppm)
Er	<1	Yb	<2	O	434(41)[d]
N	24(2)	H	525(3)	C	211(15)
F	<25(3)				

[a]Only these elements with atomic or Wt. ppm > 1 are listed.

[b]Elements from Fe to Pr were analyzed by spark source mass spectrometer (in atomic ppm).

[c]Elements from O to F were analyzed by Vacuum fusion (in Wt. ppm).

[d]Uncertainties.

There were no reactions observed between the sample and the Knudsen cell. The temperatures were measured using an optical pyrometer.

Sample Characterization

Guinier x-ray powder diffraction

The phase analysis of the samples was performed by the x-ray powder diffraction technique. The sample was ground, mixed with silicon powder (NBS Standard Reference Material 640a) and loaded in a sample holder by sticking on scotch tape. The x-ray powder pattern was taken on an Enraf-Nonius Guinier camera using nickel filtered Cu K_α (λ = 1.54056Å) radiation. The powder pattern was calibrated by using five standard silicon lines as reference.

Chemical analysis

The composition of the rare-earth sulfides was determined by the complexometric method. The sample was dissolved in diluted HCl solution and the content of rare-earth element was titrated by EDTA. The concentration of EDTA was determined previously by titrating a known amount of rare-earth metal which was dissolved in dilute HCl solution. Xylonel orange (0.2%) was used as an indicator, HMTA-NH_4OH (Ames Laboratory materials preparation

center, analytical services) or Disodium Ethylenediamine Tetracetate (titration analysis by the author) as a buffer, and the pH values were kept in the range 5-6 during the titration. The sulfur content was obtained from the difference between the weights of the total sample and the rare-earth element. For some samples, the sulfur contents were also determined by Ames Laboratory analytical services using a gravimetric method, i.e.; the rare-earth sulfide was reduced by I_3^-, then S was oxidized to SO_2 by oxygen, and finally precipitated as $BaSO_4$. The weight of S was deduced from the weight of $BaSO_4$.

Knudsen Effusion Mass-loss And Mass-spectrometric Technique

The apparatus used in our thermodynamic study is called CASMLMS (Computer Assisted Simultaneous Mass-loss and Mass-spectrometric Apparatus), which was constructed by former members of our group.[12,13] A schematic diagram of this apparatus is shown in Figure 1. The principal elements inside the stainless steel vacuum chamber are: a Cahn-RH microbalance with sensitivity better than 0.1mg which is used to monitor the mass-loss of the sample; a tungsten Knudsen cell with a knife-edge orifice on the bottom hanging on the left arm of the microbalance (the sample is placed in several semitoroidal tungsten liners and contained in

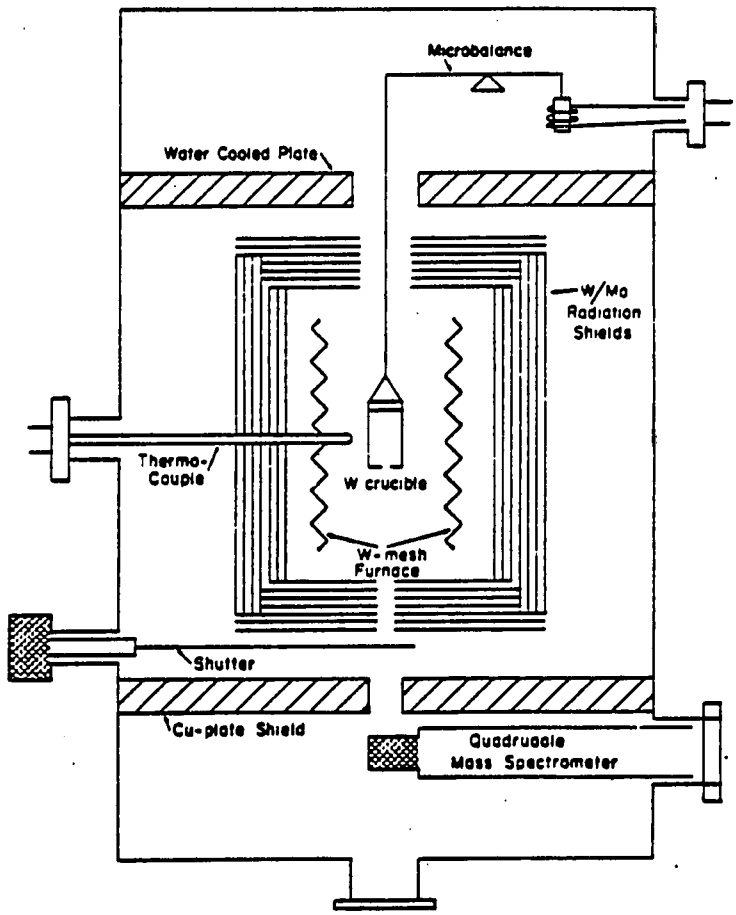

Figure 1. Schematic diagram of the simultaneous mass-loss and mass-spectrometric apparatus

Knudsen cell); a W/Mo radiation shielded tungsten mesh furnace driven by a EMI 10 Kw DC powder supply; a motor-driven shutter; a tantalum-sheathed W/5%Re - W/26%Re thermocouple with the junction located within 1/4" from the Knudsen cell (The thermocouple was previously calibrated against another thermocouple suspended vertically into the center of a dummy cell); a UTI 1-400 amu quadrupole mass-spectrometer. The vacuum system is pumped by a liquid nitrogen trapped Varian 4" diffusion pump. The residual pressure is as low as $1x10^{-7}$ Torr. The temperature is controlled by a Leeds and Northrup Electromax temperature controller which is located outside the vacuum chamber. The whole system is controlled by a computer.

Single Crystal x-ray Diffraction

The single crystal data were collected on a CAD 4B diffractometer (Enraf Nonius, Delft) for Tm_8S_{11}, and a RIGAKU AFC6R rotating anode four-circle single crystal diffractometer for $Tm_{15}S_{22}$. Details are described in sections on the corresponding compounds.

High-temperature x-ray Powder Diffraction

The phase transition of $Yb_{0.877}S(s)$ was studied by a Rigaku θ-θ high-temperature powder diffractometer with Cu Kα radiation (graphite monochromator in incident beam). The sample was contained in a Bühler chamber consisting of a cylindrical, doubled-walled and water cooled stainless steel pot with a beryllium window. Two pairs of electrodes were carried into the chamber and connected to the Mo sample holder to heat the sample holder directly. Temperatures were controlled by a high-temperature power supply from room temperature up to 2000°C. A nitrogen gas filled glove box was connected to the chamber to protect the sample and chamber from the oxygen and moisture. The chamber was baked before the temperature was raised and the diffraction data were taken. The residual pressure of the chamber held as low as 10^{-8} torr by a turbomolecular pump.

The diffraction data were collected on θ-θ stepscan mode and the step size was 0.02° in 2θ. The counting times used were 960, 360 or 120 seconds per degree(θ). The phase transition temperature was determined by observing the diffraction pattern changes as the temperature changes.

THEORY

Knudsen Effusion Mass-loss

The Knudsen effusion mass-loss method was used in our thermodynamic study. It is a method to determine partial vapor pressures by measuring the rates at which vapor species effuse through a small knife-edged orifice in an isothermal Knudsen cell containing a condensed sample in equilibrium with the vapor species. The method was named after Knudsen who first established the molecular-effusion formula and its applicability to the measurement of small vapor pressures.[14,15] It is based on the kinetic theory of the dilute gases. The molecular flux at a boundary can be calculated for a gas at equilibrium as:

$$Z_e = \frac{\nu \bar{c}}{4} \tag{1}$$

where Z_e is the molecular flux density at a boundary A_0 (in this case, it is the orifice area of the container); ν is the uniform molecular density; $\bar{c}$ is the average thermal speed of the molecules in the equilibrium gas.

According to the dilute gas theory,

$$\bar{c} = \left(\frac{8kT}{\pi m}\right)^{1/2} \tag{2}$$

$$\nu = \frac{P}{kT} \tag{3}$$

$$Z_e = \frac{1}{A_0 m} \frac{\Delta m}{\Delta t} \tag{4}$$

where m, P are the mass and pressure of the particular gaseous species, k is the Boltzmann constant and $\Delta m/\Delta t$ is the mass rate at which the particular gaseous species effuse through the orifice.

By combining equations (1) through (4), the following equation can be obtained:

$$P = \frac{1}{A_0} \frac{\Delta m}{\Delta t} \left(\frac{2\pi kT}{m}\right)^{1/2} \tag{5}$$

This equation is called the Knudsen equation, which connects the vapor pressure of a particular gaseous species over the condensed phase to its mass rate of effusion, its temperature and the orifice area of the container.

The Knudsen effusion equation (equation 5) is a valid relation for equilibrium partial pressures when the following conditions are met: (1) the vapor pressures of the effusing gases are sufficiently low so that the behavior of the effusing gases is in the molecular flow regime for which the equations (1) to (4) are valid (Knudsen found that this condition is met when the mean free path of the effusing molecule is ten times larger than the orifice diameter). (2) The rate of vapor flowing through the

orifice must be significantly lower than the gross rate of vaporization of the condensed phase so that the solid and its surface are essentially in equilibrium with the vapor, and thus equilibrium between condensed phase and vapor phase is essentially established inside the Knudsen cell. These conditions insure that the effusion rate is independent of the detailed mechanism of the vaporization process. In the experiment, this condition is frequently tested by examining the effect of varying orifice area upon vaporization rate. If the ratio of vaporization rate to the orifice area is independent of orifice area, it can be assumed that this condition is met. (3) The crucible must be maintained in a constant, uniform temperature. (4) The container must be inert to the sample and environment. (5) The orifice is knife-edged. Because such an orifice is difficult to machine in practice, the resulting orifice is more like a cylindrical channel. In this case, molecules not traveling parallel to the axis may strike the orifice wall and be returned to the cell, rather than pass through after the collision. The measured mass-loss is thus less than that expected for the vapor pressure in the Knudsen cell. A correction term called Clausing factor (W) must be used, and the Knudsen effusion cell equation is expressed as:

$$P = \frac{1}{A_0 W} \frac{\Delta m}{\Delta t} \left(\frac{2\pi kT}{m}\right)^{1/2} \tag{6}$$

For the cylindrical orifice, the Clausing factor is a function of l/r (where l and r are the length and radius of the orifice) and has been tabulated by Dushman and Lafferty.[16] When the orifice is ideal, i.e., the orifice is knife-edged, the Clausing factor W equals 1 and equation (6) reduces to equation (5).

Thermodynamic Data Analysis

In vaporization studies, two methods are used to obtain thermodynamic quantities: they are called the second-law and third-law methods. Both methods involve a term called free energy function which is defined as:

$$\text{fef}_T = \frac{G_T^\circ - H_{298}^\circ}{T}$$

$$= \frac{H_T^\circ - H_{298}^\circ}{T} - S_T^\circ \tag{7}$$

For a given reaction, the free energy function change can be written as:

$$\Delta fef_T = \frac{\Delta G^\circ_T}{T} - \frac{\Delta H^\circ_{298}}{T}$$

$$= -RLnK - \frac{\Delta H^\circ_{298}}{T} \qquad (8)$$

Thus, ΔH°_{298} can be obtained from the slope resulting from the plot of $-(\Delta fef_T + RLnK)$ vs T^{-1}. This is the second-law method which depends only on the 0th, 1st and 2nd laws of thermodynamics. Only entropy differences, and not the absolute entropies enter the calculation.

The third-law method allows the calculation of ΔH°_{298} for each measurement for the reaction by: $\Delta H^\circ_{298} = -T(\Delta fef_T + RLnK)$. An average value can be obtained from all the ΔH°_{298} values. This method is based on the knowledge of the absolute entropy of the reactants and products of the reaction.

The third-law method is generally considered superior to the second-law method if the free energy functions are known with sufficient accuracy. For most compounds, however, the free energy functions are not available and the fef's must be estimated. This is one reason that a third-law calculation is always accompanied by a second-law treatment of the same set data. Since each ΔH°_{298} value obtained by the third-law method is independent of the others, it can reveal nonequilibrium conditions during the experiment if the ΔH°_{298} values increase or

decrease with temperature change. The constancy of the third-law ΔH°_{298}'s and the agreement of ΔH°_{298} values obtained by the two methods are criteria for the acceptance or rejection of the determined values. In this work, both second- and third-law methods were used and the results were compared.

SECTION I. HIGH TEMPERATURE VAPORIZATION AND THERMODYNAMICS OF THE Nd-S SYSTEM

REVIEW OF PREVIOUS WORK

There are four solid neodymium sulfide phases between 0 and 60 at.% S: NdS, Nd_3S_4, Nd_5S_7 and Nd_2S_3. Structural data for these solids have been tabulated in Pearson's handbook[1] and are shown in Table 1.1 here. Among them, Nd_2S_3 exhibits two polymorphic structures in different temperature ranges. The transformation of Nd_2S_3 between these two polymorphic structures was found by Besancon[2] to occur at 1180°C. α-Nd_2S_3 is the low temperature form and γ-Nd_2S_3 is the high temperature form. Besides the two Nd_2S_3 polymorphic structures, a β-phase has been reported. The results reported concerning the structure of this phase are a matter of controversy. Besancon and coworkers[3] detected a β-phase for Nd_2S_3. Prewitt and Sleight[4] denied the existence of this phase. Eliseev et al.[5] described β-Nd_2S_3 as a cubic structure with a unit cell parameter a = 19.87Å and space group $Fd\bar{3}m$. They did not report the atomic positions. Later, Besancon[2] reported that the true β sesquisulfide phase exists only with lanthanum and that the β-phase of neodymium is a solid solution with the formula $Nd_{10}S_{14}O_xS_{1-x}$ ($x>0$) and space group $I4_1/acd$. It seems from this paper that the previously reported Nd_5S_7[6] does not exist, its formula is actually $Nd_{10}S_{14}O_xS_{1-x}$. He also found that this oxysulfide lose oxygen at high temperature and transforms into a γ sulfide with the Nd_5S_7 composition.

Table 1.1. Crystallographic data for Nd-S system

PHASE	STRUCTURE TYPE	SPACE GROUP	LATTICE PARAMETERS			REFERENCE
			a(Å)	b(Å)	c(Å)	
NdS	NaCl	$Fm\bar{3}m$	5.6952			7,8
Nd_3S_4	Th_3P_4	$I\bar{4}3d$	8.524			9,10
Nd_5S_7	Ce_5S_7	$I4_1/acd$	14.94		19.82	6
$Nd_2S_3(\gamma)$	Th_3P_4	$I\bar{4}3d$	8.527			11
$Nd_2S_3(\alpha)$	La_2S_3	Pnma	7.442	4.029	15.519	12
Nd_2S_3	unknown	$Fd\bar{3}m$	19.87			5

Both Nd_3S_4 and Nd_2S_3 have the Th_3P_4 type structure. It has been reported by Flahaut et al.[13] that a complete solid solution exists between Nd_3S_4 and Nd_2S_3 and the reported unit cell parameters are practically identical.

NdS crystallizes in the B1 structure (NaCl type) with a wide homogeneity range. Guittard[14] and Flahaut et al.[15] evaluated the extent of the homogeneity regions of the whole series of rare-earth monosulfides on the basis of x-ray phase analysis and lattice parameter measurements. In the case of neodymium, the region of homogeneity extends from NdS to $NdS_{0.75}$ with little change in lattice parameter (5.685 - 5.682Å). However, Bruzzone and Olcese[8] provided information indicating an appreciable change in the lattice parameter (5.693 - 5.680Å) for the neodymium monosulfide and a homogeneity region from NdS to $NdS_{0.77}$. A dependence of the extent of the homogeneity region on the temperature has been reported by both groups.

A thermal investigation conducted by Picon et al.[16] showed that Nd_2S_3 has a low rate of evaporation and negligible dissociation up to 2000°C; and Nd_3S_4 has even less tendency to dissociate; noticeable dissociation and conversion to the monosulfide in Nd_3S_4 was observed only at temperatures close to its melting point (2040°C) upon prolonged heating under vacuum.

Thermodynamic measurements on NdS, Nd_2S_3 and Nd_3S_4 solids have been done both calorimetrically and mass-spectrometrically. Bayanov[17] reviewed these studies. Most of the data in Table 1.2 are cited from his review. Among them, the enthalpies of formation of Nd_2S_3 obtained by several workers are in poor agreement. The only data available on the enthalpy of formation of Nd_3S_4 was obtained by the calorimetric method, no details of vaporization reactions and partial pressures of gaseous species have been reported.

Table 1.2. Enthalpies of formation and dissociation energies of neodymium sulfides

Compound	$-\Delta H^{\circ}_{f(298)}$ (kcal mole^{-1})	D°_{298} (kcal mole^{-1})	D°_{0} (kcal mole^{-1})
NdS(g)	111±1	113	112.2±3.5[18]
	104.8	118.1	
	108.5		
Nd_2S_3(s)	269±3		
	285.9		
	277		
Nd_3S_4	388.0		

All the data are cited from ref. 17 unless otherwise noted.

EXPERIMENT

Vaporization Study

Samples with compositions in the range $1.0 \leq S/Nd \leq 1.5$ were induction heated under vacuum in the temperature range 1600°C - 1900°C for several hours until more than 20% of the sample vaporized. In all cases, the final residues were black colored samples. X-ray powder diffraction and chemical analysis showed that the black residues were single phase $Nd_{3-x}S_4$. Chemical analysis shows that the compositions are between $NdS_{1.36(\pm 0.02)}$ and $NdS_{1.40(\pm 0.02)}$. The average composition $NdS_{1.38}$ was used to calculate the thermodynamic properties from the mass-loss Knudsen effusion measurement. The gaseous species over the congruently vaporizing phase $Nd_{3-x}S_4(s)$ were determined mass-spectrometrically to be: neodymium monosulfide, atomic neodymium and atomic sulfur. It was concluded that $NdS_{1.38}$ vaporizes congruently according to:

$$NdS_{1.38}(s) = NdS(g) + 0.38\ S(g) \qquad (1.1)$$

$$NdS_{1.38}(s) = Nd(g) + 1.38\ S(g) \qquad (1.2)$$

Mass-loss Knudsen Effusion Experiment

The mass loss rates were measured during the congruent vaporization of $NdS_{1.38}(s)$ on the CASMLMS apparatus. Four series of experiments were performed with 90, 133, 73, 68 mg $NdS_{1.38}(s)$ samples over temperature range 1952 - 2229 K. The orifice areas of the Knudsen cells used in the experiments were 1.29×10^{-2} and 8.81×10^{-3} cm^2.

RESULTS

The partial pressures of Nd(g), S(g), NdS(g) were obtained by using the following three equations:

(1) Knudsen effusion equation:

$$\frac{\Delta m}{\Delta t} = \frac{A_0}{3.76\times10^{-7}T^{1/2}}[(M_{Nd})^{1/2}P_{Nd}+(M_S)^{1/2}P_S+(M_{NdS})^{1/2}P_{NdS}] \quad (1.3)$$

where $\Delta m/\Delta t$ is mass loss rate in mg/min and A_0 is the Knudsen cell orifice area in cm^2.

(2) Congruent vaporization condition:

$$\frac{P_{Nd}}{(M_{Nd})^{1/2}}+\frac{P_{NdS}}{(M_{NdS})^{1/2}}=\frac{1}{1.38}\left[\frac{P_S}{(M_S)^{1/2}}+\frac{P_{NdS}}{(M_{NdS})^{1/2}}\right] \quad (1.4)$$

(3) Gas phase equilibrium constant:

$$K = \frac{P_S\,P_{Nd}}{P_{NdS}} \quad (1.5)$$

Here $LnK = -\Delta G^\circ_{diss}/RT$, where ΔG°_{diss} is the standard free energy change associated with the dissociation of NdS(g). It was obtained at various temperatures using the value $D^\circ_0 = 112.2(\pm3.5)$ kcal $mole^{-1}$ for NdS(g)[18] together with enthalpy increments and entropies for NdS(g) from Mills' compilation,[19] S(g) from the JANAF Tables,[20] Nd(g) from Hultgren et al.[21]

In this work, 87 mass-loss vs temperature data points were measured in four independent mass loss experiments. The mass loss rate at each temperature, the partial pressures of neodymium, sulfur and neodymium monosulfide are listed in Tables 1.3 - 1.6. The resulting individual pressures of gas phase species were treated by unweighted linear-least squares (Figures 1.1 - 1.3) to give:

$$\mathrm{Ln}P_{S}\ (\mathrm{atm}) = -\ 63373(\pm 439)/T + 15.67(\pm 0.21) \qquad (1.6)$$

$$\mathrm{Ln}P_{Nd}\ (\mathrm{atm}) = -\ 62802(\pm 368)/T + 15.64(\pm 0.18) \qquad (1.7)$$

$$\mathrm{Ln}P_{NdS}\ (\mathrm{atm}) = -\ 66285(\pm 807)/T + 17.09(\pm 0.39) \qquad (1.8)$$

The second law enthalpies and entropies of the vaporization reactions: $NdS_{1.38}(s) = NdS(g) + 0.38\ S(g)$ (I), $NdS_{1.38}(s) = Nd(g) + 1.38\ S(g)$ (II) were obtained by plotting - RLnK vs T^{-1} for all the experimental data to obtain the slopes and intercepts which yield the enthalpies and entropies at the median temperature. The median thermodynamic values were reduced to 298K, utilizing the thermal functions of S(g)[20], Nd(g)[21] and NdS(g).[19] The thermal functions for $NdS_{1.38}(s)$ were estimated using Kubaschewski's approximation.[22] The heat capacity of $NdS_{1.38}(s)$ thus obtained is:

$$C_P = 16.83 + 3.633\times10^{-4} - 2.333\times10^{5}T^{-2} \qquad (1.9)$$

Maximum errors of ±1 kcal $mole^{-1}$ in the enthalpy function and ±1 cal $mole^{-1}$ K^{-1} in the entropy are assumed to result from use

Table 1.3. First run data and results
Orifice area = 1.29×10^{-2} cm

T (K)	$\Delta m/\Delta t \times 10^2$ (mg/min)	$P_S \times 10^7$ (atm)	$P_{Nd} \times 10^7$ (atm)	$P_{NdS} \times 10^7$ (atm)	ΔH°_{298}(I) (kcal/mole)	ΔH°_{298}(II) (kcal/mole)
2180	3.62	14.1	18.7	14.7	189.9	302.8
2129	1.86	7.22	9.26	7.34	189.8	302.7
2105	1.31	5.11	6.58	5.10	189.9	302.8
2080	0.953	3.67	4.71	3.71	189.5	302.4
1978	0.236	0.874	1.11	0.922	188.4	301.3
2029	0.457	1.74	2.25	1.74	189.3	302.3
2204	5.05	19.7	25.2	20.9	189.8	302.7
2229	8.04	30.5	38.0	35.9	188.6	301.5
2214	6.55	24.9	31.2	28.8	188.8	301.7
2199	5.40	20.5	25.7	23.6	188.8	301.7
2008	0.319	1.23	1.59	1.18	189.6	302.5
2179	4.12	15.7	19.7	17.8	188.8	301.7
2163	3.34	12.7	16.0	14.2	188.8	301.8
2148	2.86	10.7	13.4	12.3	188.5	301.4
2134	2.14	8.19	10.4	8.84	189.1	302.0
2119	1.79	6.78	8.59	7.38	189.0	301.9

Table 1.4. Second run data and results
Orifice area = $1.29 \times 10^{-2} cm^2$

T (K)	$\Delta m/\Delta t \times 10^2$ (mg/min)	$P_S \times 10^7$ (atm)	$P_{Nd} \times 10^7$ (atm)	$P_{NdS} \times 10^7$ (atm)	ΔH°_{298}(I) (kcal/mole)	ΔH°_{298}(II) (kcal/mole)
2121	1.57	6.16	7.96	6.05	190.1	303.0
2138	2.09	8.13	10.4	8.31	189.8	302.7
1953	0.12	0.468	0.619	0.403	190.3	303.2
2150	2.37	9.29	12.0	9.34	190.0	302.9
2169	3.10	12.2	15.6	12.4	190.0	302.9
2189	4.33	16.8	21.3	18.1	189.5	302.4
2069	0.85	3.24	4.15	3.35	189.2	302.1
2055	0.679	2.59	3.33	2.64	189.3	302.2
2102	1.20	4.70	6.10	4.53	190.2	303.1
1954	0.126	0.489	0.644	0.431	190.1	303.0
1994	0.272	1.03	1.33	1.02	189.2	302.1
2013	0.356	1.36	1.76	1.34	189.4	302.3
2036	0.486	1.88	2.43	1.81	189.7	302.6

Table 1.5. Third run data and results
Orifice area = $1.29 \times 10^{-2} cm^2$

T (K)	$\Delta m/\Delta t \times 10^2$ (mg/min)	$P_S \times 10^7$ (atm)	$P_{Nd} \times 10^7$ (atm)	$P_{NdS} \times 10^7$ (atm)	ΔH°_{298}(I) (kcal/mole)	ΔH°_{298}(II) (kcal mole)
2055	0.82	3.01	3.77	3.47	188.0	300.9
2149	2.91	10.9	13.7	12.6	188.5	301.9
2030	4.95	1.87	2.39	1.94	188.9	301.8
2127	1.99	7.57	9.58	8.26	189.0	301.9
2078	0.933	3.59	4.61	3.63	189.5	302.4
2102	1.37	5.23	6.66	5.53	189.2	302.1
2089	1.00	3.92	5.09	3.76	190.2	303.1
2016	0.337	1.32	1.72	1.20	190.2	303.1
2134	2.27	8.57	10.8	9.61	188.7	301.6
2031	0.444	1.72	2.23	1.64	189.8	302.7
2112	1.65	6.24	7.89	6.84	188.9	301.8
2053	0.60	2.34	3.04	2.23	190.0	302.9
2153	2.71	10.4	13.3	11.1	189.4	302.3
1998	0.326	1.21	1.53	1.30	188.3	301.2
2176	3.43	13.4	17.2	13.9	189.9	302.8
1991	0.266	0.100	1.29	1.01	189.0	301.9

Table 1.5. (Continued)

T (K)	$\Delta m/\Delta t \times 10^2$ (mg/min)	$P_S \times 10^7$ (atm)	$P_{Nd} \times 10^7$ (atm)	$P_{NdS} \times 10^7$ (atm)	ΔH°_{298}(I) (kcal/mole)	ΔH°_{298}(II) (kcal/mole)
2059	0.732	2.79	3.57	2.87	189.2	302.1
2199	4.73	18.5	23.5	19.6	189.7	302.6
2042	0.476	1.88	2.46	1.69	190.5	303.4
2007	0.314	1.21	1.57	1.15	189.7	302.6
1982	0.195	0.760	1.00	0.677	190.2	303.1
2105	1.44	5.49	6.99	5.84	189.1	302.0
1971	0.214	0.791	1.01	0.837	188.3	301.2
2072	0.796	3.11	4.03	2.98	190.1	303.0
2057	0.591	2.33	3.06	2.12	190.5	303.4
1956	0.111	0.444	0.60	0.349	191.3	304.2
1966	0.167	0.638	0.832	0.601	189.5	302.4
2180	3.67	14.3	18.3	15.0	189.8	302.6
2141	2.07	8.15	10.5	8.04	190.2	303.1
2104	1.31	5.08	6.53	5.12	189.7	295.2
1952	1.43	0.539	0.697	0.527	189.0	301.9

Table 1.6. Fourth run data and results
Orifice area = $8.81 \times 10^{-3} cm^2$

T (K)	$\Delta m/\Delta t \times 10^2$ (mg/min)	$P_S \times 10^7$ (atm)	$P_{Nd} \times 10^7$ (atm)	$P_{NdS} \times 10^7$ (atm)	ΔH°_{298}(I) (kcal/mole)	ΔH°_{298}(II) (kcal/mole)
2019	0.283	1.56	2.00	1.61	189.0	301.9
2038	0.385	2.12	2.71	2.23	188.9	301.8
2093	0.840	4.68	5.95	4.98	189.1	302.0
2112	1.20	6.57	8.23	7.48	188.4	301.3
1993	0.20	1.09	1.39	1.14	188.6	301.5
2056	0.478	2.67	3.42	2.73	189.3	302.2
2074	0.612	3.43	4.40	3.51	189.4	302.3
2127	1.31	7.36	9.38	7.80	189.3	302.2
2145	1.70	9.53	12.1	10.3	189.2	302.1
2015	0.235	1.33	1.74	1.25	189.9	302.8
2181	2.73	15.4	19.4	16.8	189.2	302.1
2110	0.93	5.33	6.88	5.23	190.0	303.0
2163	2.21	12.4	15.6	13.7	189.0	301.9
2064	0.473	2.71	3.53	2.56	190.2	303.1
2118	1.14	6.44	8.21	6.77	189.3	302.2
2152	1.88	10.5	13.3	11.5	189.1	302.0

Table 1.6. (Continued)

T (K)	$\Delta m/\Delta t \times 10^2$ (mg/min)	$P_S \times 10^7$ (atm)	$P_{Nd} \times 10^7$ (atm)	$P_{NdS} \times 10^7$ (atm)	ΔH°_{298}(I) (kcal/mole)	ΔH°_{298}(II) (kcal/mole)
2136	1.59	8.80	11.1	9.84	188.7	301.7
2124	1.29	7.21	9.16	7.75	189.1	302.0
2042	0.387	2.16	2.77	2.19	189.2	302.1
2086	0.752	4.19	5.33	4.43	189.1	302.0
2100	0.962	5.31	6.71	5.83	188.8	301.7
2000	0.224	1.22	1.56	1.29	188.6	301.5
2051	0.442	2.47	3.17	2.51	189.3	302.2
2109	1.05	5.86	7.44	6.27	189.1	302.0
2184	2.78	15.7	19.9	17.0	189.4	302.3
2150	1.93	10.7	13.5	12.0	188.8	301.7
2078	0.697	3.85	4.89	4.15	188.8	301.7

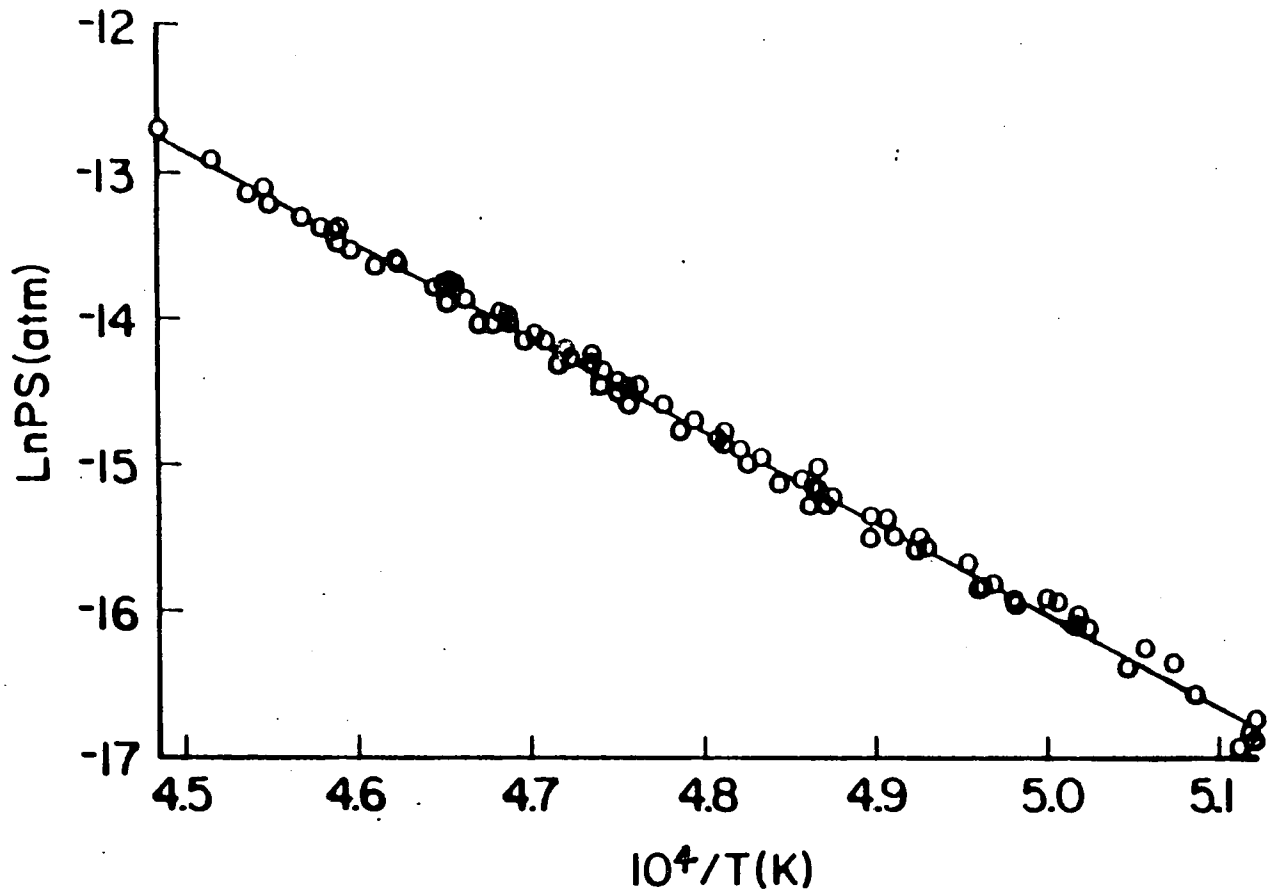

Figure 1.1 Second-law plot, LnP_S (atm) vs. 1/T (K)

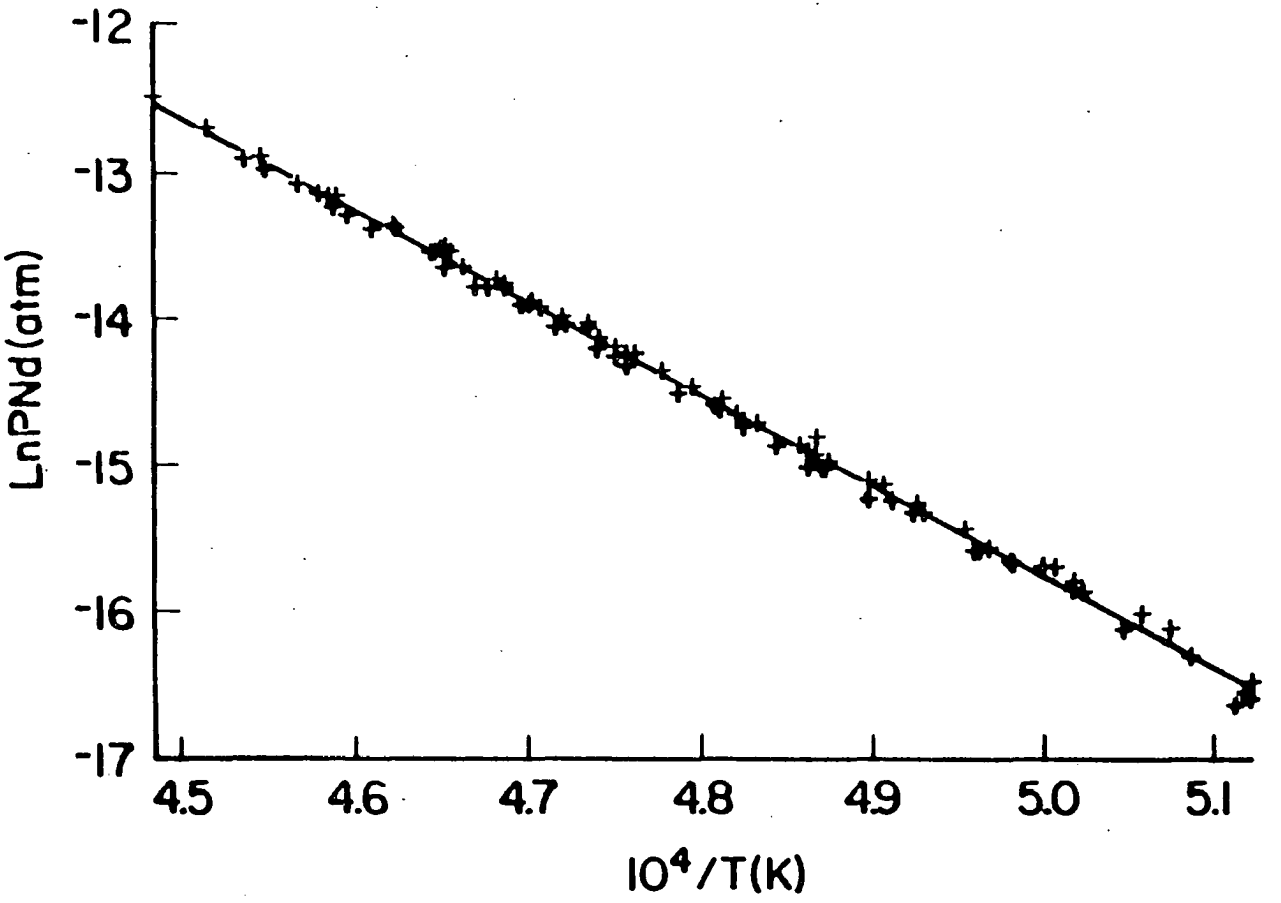

Figure 1.2 Second-law plot, LnP_{Nd} (atm) vs. 1/T (K)

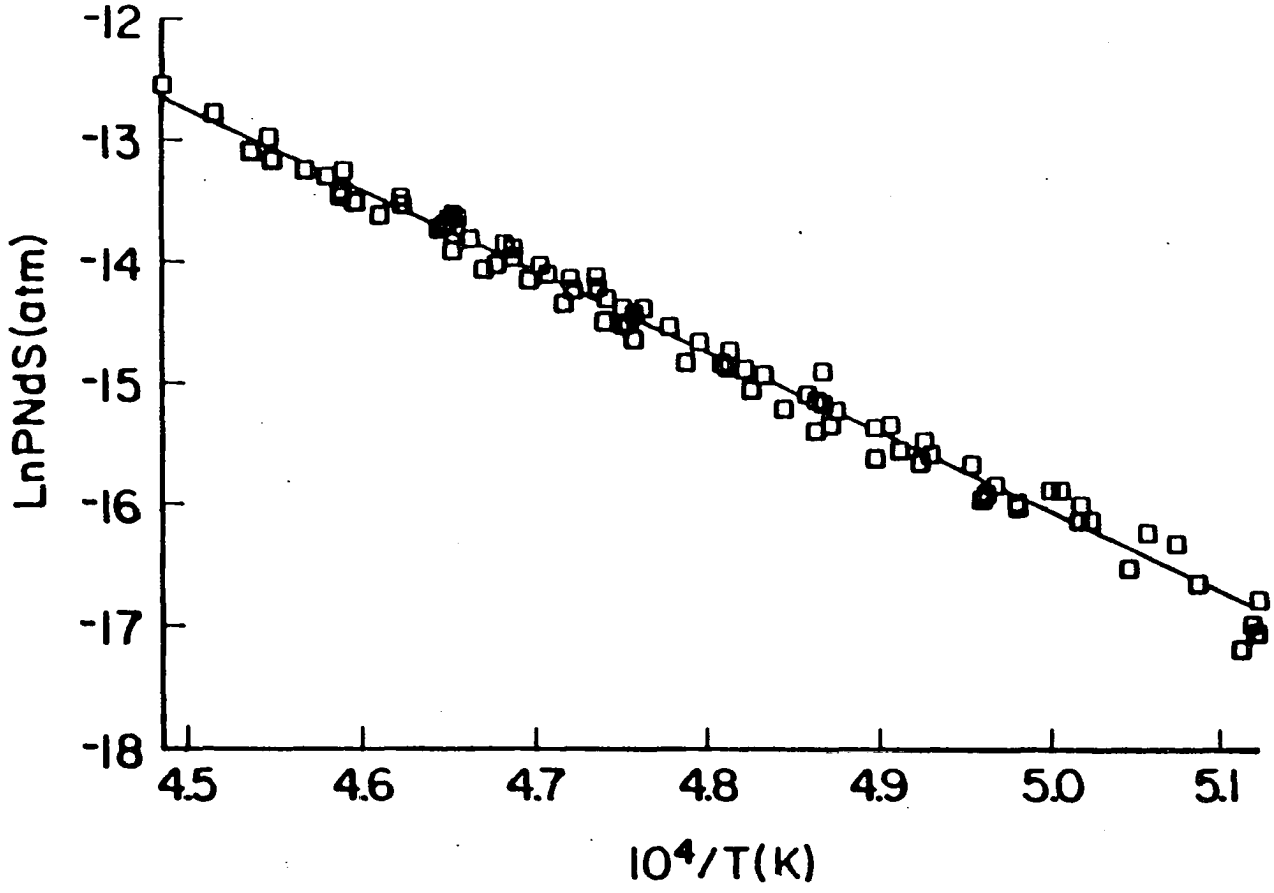

Figure 1.3 Second-law plot, LnP_{NdS} (atm) vs. 1/T (K)

this equation. The standard entropy of $NdS_{1.38}(s)$ was estimated to be 20.7±1.0 cal $mole^{-1}$ K^{-1} by comparing with the standard entropies of NdS(s), $Nd_2S_3(s)$, $Pr_3S_4(s)$, $Ce_3S_4(s)$ etc.[19] The third law enthalpies were obtained by a point-by-point evaluation of -T(RLnK + Δfef). The resulting second- and third-law enthalpies and entropies are listed in Table 1.7.

Table 1.7. Thermodynamic results for $NdS_{1.38}(s)$

Reactions	3rd-law		2nd-law	
	ΔH°_{298} (kcal mole^{-1})	[a] ΔS°_{298} (cal mole^{-1}K^{-1})	ΔH°_{298} (kcal mole^{-1})	ΔS°_{298} (cal mole^{-1}K^{-1})
[b] (I)	189.4 (±2.0)	57.8 (±1.0)	191.6 (±4.0)	58.8 (±2.0)
[b] (II)	302.3 (±2.0)	79.9 (±1.0)	304.5 (±4.0)	81.8 (±2.0)

[a] Calculated from reference data.

[b] (I) corresponds to reaction (1.1).

(II) corresponds to reaction (1.2).

DISCUSSION

Unlike the Pr-S system in which both PrS(s) and Pr_3S_4(s) vaporize congruently,[23] in the Nd-S system only $Nd_{3-x}S_4$ ($0.06 \leq x \leq 0.14$) vaporizes congruently. It was found in the vaporization studies above 1700°C that NdS(s) lost Nd(g) preferentially to yield $Nd_{3-x}S_4$.

The enthalpy of the dissociation of $Nd_{2.9}S_4$(s) is obtained by combining the following equations:

$2.9Nd(g)+4S(g)=Nd_{2.9}S_4(s)$ $\Delta H^\circ_{298} = -876.7\pm4.0$ kcal/mole (1.10)

(3rd-law result)

$Nd(s) = Nd(g)$ $\Delta H^\circ_{298} = 78.3$ kcal/mole[21] (1.11)

$S(Rh) = S(g)$ $\Delta H^\circ_{298} = 66.2$ kcal/mole[20] (1.12)

Adding (1.10) + 2.9x(1.11) + 4x(1.12) yield:

$2.9Nd(s)+4S(Rh)=Nd_{2.9}S_4(s)$ $\Delta H^\circ_{298(f)} = -385\pm4.0$ kcal/mole (1.13)

(3rd-law result)

Finogenov[17] obtained $\Delta H^\circ_{298(f)} = -388$ kcal mole^{-1} for Nd_3S_4(s) by the calorimetric method. Since the congruently vaporizing compounds in our experiment were not exactly stoichiometric, the difference between these results, although within the estimated uncertainties, is understandable.

Fenochka[24] measured the thermodynamic properties of $Nd_2S_3(s)$ over the temperature range 1855 - 2320K by the mass spectrometric method. It was found in our experiment that in the above temperature range, $Nd_2S_3(s)$ vaporizes incongruently and the solid phase becomes single phase $Nd_{3-x}S_4(s)$ which vaporizes congruently. Thus the previously reported results are probably more appropriate to $Nd_{3-x}S_4$. The Th_3P_4-type phase has a homogeneous range between Nd_3S_4 and Nd_2S_3 at high temperatures. Chemical analysis is necessary because the composition of the solid phase cann't be determined by only using X-ray diffraction analysis.

In this work, it was found that either $Nd_{1.38\pm0.02}$ vaporizes congruently or the congruently vaporizing composition varies between $NdS_{1.36}$ to $NdS_{1.40}$. However, uncertainties in the chemical analysis did not allow a distinction to be made between these alternatives. The two alternatives yield the same calculated enthalpies to well within the quoted uncertainties.

REFERENCES

1. Villars, P.; Calvert, L. D. Pearson's Handbook of Crystallographic Data for Intermetallic Phases; American Society of Metals: Metals Park, Ohio, 1985.

2. Besancon, P. J. Solid State Chem., 1973, 7, 232.

3. Besancon, P.; Adolphe, C.; Flahaut, J. Compt. Rend. Ser. C, 1968, 266, 111.

4. Prewitt, C. P.; Sleight, A. W. Inorg. Chem., 1968, 7, 1090.

5. Eliseev, A. A.; Uspenskaya, S. I.; Fedorov, A. A. Russ. J. Inorg. Chem., 1970, 15(7), 1036.

6. Besancon, F.; Picon, M. C. R. Acad. Sci. Ser.C, 1968, 267, 1130.

7. Hulliger, F.; Landolt, M.; Schmelczer, R.; Zarbach, I. Solid State Communications, 1975, 17, 751.

8. Bruzzone, G.; Olcese, G. L. Proprietes Thermodynamiques Physiques et Structurales des Derives Semi-metalliques, Colloques Internationaux du Centre National de la Recherche Scientifique, Orsay, 1965, p 387.

9. Zhuze, V. P.; Sergeeva, V. M.; Golikova, O. A. Soviet Phys. Solid State, 1970, 11, 2071.

10. Kupriyanov, B. A.; Pechennikov, A. V.; Uspenskaya, S. I.; Eliseev, A. A.; Chechernikov, V. I. Russ. J. Inorg. Chem., 1977, 22(5), 768.

11. Picon, M.; Flahaut, J. Compt. Rend., 1956, 243, 2074.

12. Eliseev, A. A.; Uspenskaya, S. I.; Fedorov, A. A.; Tolstova, V. A. J. Struc. Chem.(Eng. Tran.), 1972, 13, 66.

13. Flahaut, J.; Guittard, M.; Patrie, M.; Pardo, M.; Golabi, S. M.; Domange, L. Acta Cryst., 1965, 19, 14.

14. Guittard, M. C. R. Acad. Sci. Ser. C, 1965, 261, 2109.

15. Flahaut, J.; Guittard, M.; Gorochov, O. Colloq. int. CNRS, 1965, 157, 431.

16. Picon, M.; Domange, L.; Flahaut, J.; Guittard, M.; Patrie, M. Bull. Soc. Chim. France, 1960, 2, 221.

17. Bayanov, A. P. Russ. Chem. Rev., 1975, 44, 122.

18. Smoes, S.; Coppens, P.; Bergman, C.; Drowart, J. Trans. Faraday Soc., 1969, 65, 682.

19. Mills, K. C. Thermodynamic data for Inorg. Sulphides, Selenides and Tellurides; Butterworths: London, 1974.

20. Chase, M. W. Jr.; Davies, C. A.; Downey, J. R.; Frurip,D. J.; McDonald, R. A.; Syverud, A. N. JANAF Thermodynamic Tables; American Chemical Society and the American Institute of Physics for the National Bureau of Standards: Midland, 3rd edn.; 1986; p 1779.

21. Hultgren, R.; Desai, P. D.; Hawkins, D. T.; Gleiser, M.; Kelley, K. K.; Wagman, D. D.Selected Values of the Thermodynamic Properties of the Elements; American Society for Metals: Metals Park, OH, 1973; p 344.

22. Kubaschewski, O. Metallurgical Thermochemistry; Pergamon: New York, 5th edn.; 1979; p 183.

23. Cater, E. D.; Mueller, B. H.; Fries, J. A. NBS Spec. Publ, 1979, 561, 237.

24. Fenochka, B. V. Inorg. Material (English Translation), 1986, 22(10), 1520.

SECTION II. HIGH TEMPERATURE VAPORIZATION AND THERMODYNAMICS OF THE Yb-S SYSTEM

REVIEW OF PREVIOUS WORK

The structural data for the known ytterbium sulfides have been tabulated in Pearson's handbook[1] and are shown in Table 2.1. Among them, both Yb_2S_3 with the Sb_2S_3-type structure and with the Th_3P_4-type structure exist only at high temperature and high pressure. The monoclinic Yb_2S_3 (δ-phase) with space group $P2_1/m$ was obtained from a KI melts at 1000°C in an inert, CS_2 - containing atmosphere.[2] For the two Yb_2S_3 structures with Pearson symbols O** and CF*, only the lattice parameters were obtained, the structures are unsolved. Patrie[3] found that ε-Yb_2S_3 (Al_2O_3-type) forms from Yb_2O_3 and H_2S at 1000 to 1300°C. Preparation of Yb_2S_3 from the elements in evacuated quartz ampoules at 980°C also forms ε-Yb_2S_3; while between 650 and 950°C, the yellow cubic θ-Yb_2S_3 forms. The transformation of θ-Yb_2S_3 to ε-Yb_2S_3 at about 950°C to 980°C appears irreversible. According to Eliseev et al.,[4] the transformation of θ-Yb_2S_3 to ε-Yb_2S_3 occurs as low as just above 700°C. Later, Kuz'micheva[5] claimed that the so called Al_2O_3-type Yb_2S_3 is actually a structure with space group $P6_3cm$. Cubic θ-Yb_2S_3 phase was reported by Eliseev et al.[6] to be Yb_3S_5 and to form peritectically. Later, Kuz'micheva et al[7] solved the structure of θ-Yb_2S_3 and determined the composition to be Yb_2S_3 by single crystal work. They also reported that both ytterbium and sulfur positions have vacancies.

Table 2.1. Crystallographic data for Yb-S system

PHASE	STRUCTURE TYPE	SPACE GROUP	LATTICE PARAMETERS				REFERENCE
			a(Å)	b(Å)	c(Å)	BETA(DEG.)	
YbS	NaCl	$Fm\bar{3}m$	5.694				8,9
Yb_3S_4	Yb_3S_4	Pnma	12.71	3.80	12.88		13
$Yb_2S_3(\delta)$	Yb_2S_3	$P2_1/m$	18.15	4.06	10.37	100.0	2
$Yb_2S_3(\varepsilon)$	Yb_2S_3	$P6_3cm$	6.772		18.28		5,10
$Yb_2S_3(\varepsilon)$	Al_2O_3	$R\bar{3}c$	6.772		18.28		11
$Yb_2S_3(\theta)$	Mn_2O_3	$Ia\bar{3}$	12.47				3
Yb_2S_3	Sb_2S_3	Pnma	10.435	3.786	10.330		12
Yb_2S_3	Th_3P_4	$I\bar{4}3d$	8.224				13
Yb_2S_3	Unknown	O**	6.788	9.981	3.617		14
Yb_2S_3	Unknown	cF*	10.51				3,6

NaCl type (B1) ytterbium monosulfide exhibits a wide homogeneity range with cation vacancies. Its composition range, according to various authors, falls within the following limits: $YbS_{1.11}$ - $YbS_{1.14}$[15] and $YbS_{0.98}$ - $YbS_{1.08}$.[4,16] A general formula for the nonstoichiometric ytterbium monosulfide has been established by Flahaut et al.[17] to be $Yb^{3+}_{2/3x}Yb^{2+}_{1-x}S^{2-}T_{1/3x}$ (here T represents Yb vacancy) based on magnetic susceptibilities and densities. An ordered compound with composition $Yb_{0.875}S$, with doubled lattice parameter a = 2xa(B1) was discovered by Tomas et al.[18] They also suggested that the true structure is probably rhombohedral, even though the reflections could be indexed on a doubled cubic cell with space group $F\bar{4}3m$. The unique [111] axes of small rhombohedral domains were thought to be oriented in all four <111> directions of a parent cubic structure. But they found no weak satellite reflections or diffuse scattering to support this argument. In their electron diffraction study of the Yb-S system, Otero-diaz and coworkers[19] observed the rhombohedral structure and the weak satellite reflections which appear sometimes in a single direction. However they were still unable to distinguish the superstructure with a doubled cubic cell from the rhombohedral cell.

Orthorhombic Yb_3S_4 with space group Pnma has been found to have a range of homogeneity of $YbS_{1.33}$ - $YbS_{1.46}$ by Chevalier et

al.[20] and $YbS_{1.27}$ - $YbS_{1.44}$ by Eliseev et al.[6] Otero-diaz et al.[19] revealed by electron diffraction that nonstoichiometric $Yb_{3-\sigma}S_4$ was modulated in the b direction, usually incommensurately with modulation period around 7x to 8xb. They also discovered a high temperature phase of Yb_3S_4 with space group Cmcm, a new polymorphic structure of Yb_3S_4.

A phase diagram for the Yb-S system between 0 and 62.5 at.% S at 4.5 atm. was obtained by Eliseev et al.[6], and is shown in Figure 2.1. They found that both YbS and Yb_3S_4 melt congruently, at 2130 ± 50°C and 1800°C, respectively. Only one thermodynamic investigation of the Yb-S system was undertaken previously. Fenochka and Gordienko[21] obtained the dissociation energy and heat of formation of YbS(s) by the mass spectrometric method. The results were: $\Delta H^\circ_{diss(298)}$ = 199.4 ± 2.0 kcal $mole^{-1}$, $\Delta H^\circ_{f(298)}$ = -97.9 kcal $mole^{-1}$. Smoes et al.[22] estimated the dissociation energy of YbS(g) at 0K to be about 39 kcal $mole^{-1}$ by comparing with the whole series of rare-earth monoxides and monosulfides.

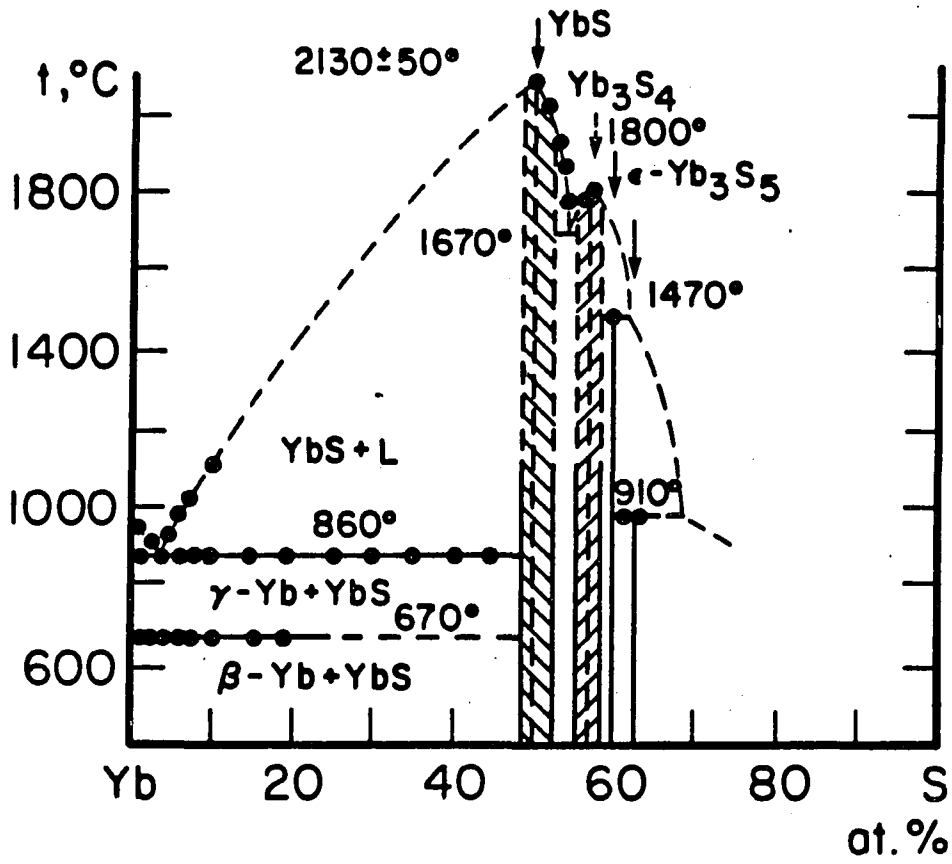

Figure 2.1 The equilibrium diagram of the Yb-S system at p=4.5 atm

EXPERIMENT

Sample Preparation and Characterization

A series of Yb - S samples with compositions in the range 0.9 $\leq$ S/Yb $\leq$ 1.5 were synthesized. For the samples with compositions of S/Yb > 1.20 the preparation method described in the experiment section was used. Samples with compositions S/Yb less than 1.20 were initially found to react with the quartz tubes to produce Yb_2O_3 when the temperature was higher than 500°C. Subsequently, for the preparation of those samples, the temperature of the quartz tube was always kept below 500°C.

Vaporization and Mass Spectrometric Study

Vaporization of all samples from a tungsten crucible heated inductively in vacuum over the temperature range 1600 - 2000 K showed that upon long-term vaporization all samples changed to a nonstoichiometric sulfur-rich monosulfide with the composition $Yb_{0.877(\pm 0.05)}S$. The composition was determined by complexometric titration (Ames Laboratory materials preparation center, analytical services). Small amounts (about 1%) of Yb_2O_2S were found to coexist with $Yb_{0.877}S$. The indications are that

oxygen has a very low solubility in the monosulfide and forms the oxysulfide when present at high temperatures. This second phase is inert so far as the vaporization reaction is concerned and, in fact, its formation serves to scavenge the oxygen. It was concluded that $Yb_{0.877}S$ vaporizes congruently. Mass spectrometric investigation showed that the only Yb containing species in the gas phase is ytterbium, and the only other species of importance are sulfur and S_2. No YbS^+, YbS_2^+, YbO^+ were observed. It was concluded that $Yb_{0.877}S$ vaporizes congruently according to :

$$Yb_{0.877}S(s) = 0.877\ Yb(g) + S(g) \qquad (2.1)$$

X-ray powder diffraction showed that $Yb_{0.877}S(s)$ has a defect ordered NaCl-type superstructure at low temperatures with doubled lattice parameter. The structure has been reported by Alain Tomas et al.[18] The phase transition of $Yb_{0.877}S$ was studied in our work by using a high temperature x-ray powder diffractometer. A first order phase transition was observed at around 1100°C, and the high temperature form was found to be the NaCl-type structure.

Mass-loss Knudsen Effusion Experiment

Mass loss measurements were performed on the CASMLMS apparatus. In the experiment, three $Yb_{0.877}S$ samples which weighed about 50, 150 and 100 mg were studied using tungsten Knudsen cells with orifice areas of 1.29×10^{-2} and $8.81 \times 10^{-3} cm^2$. The orifices were machined to a "knife edge". No correction was applied for transmission by the orifice. No evidence of interaction, either by reaction or diffusion, between the sample and the tungsten crucible was found. Small amounts of Yb_2O_2S in the initial $Yb_{0.877}S$ samples do not affect the equilibrium of reaction (2.1). The mass loss rates were measured during the congruent vaporization of $Yb_{0.877}S$ over the temperature range 1688 - 1842K.

RESULTS

The partial pressures of gas species ytterbium, sulfur and S_2 were obtained by simultaneously solving following three equations:

(1) Knudsen effusion equation:

$$\frac{\Delta m}{\Delta t} = \frac{A_0}{3.76\times10^{-7}T^{1/2}} [(M_{Yb})^{1/2}P_{Yb} + (M_S^{1/2})P_S + (M_{S_2})^{1/2}P_{S_2}] \quad (2.2)$$

(2) Congruent vaporization condition:

$$\frac{P_S}{(M_S)^{1/2}} + \frac{2P_{S_2}}{(M_{S_2})^{1/2}} = \frac{1}{0.877}\ \frac{P_{Yb}}{(M_{Yb})^{1/2}} \quad (2.3)$$

(3) The equilibrium between S(g) and S_2(g):

$$K = \frac{P_{S_2}^{1/2}}{P_S} \quad (2.4)$$

Here $\Delta m/\Delta t$ is the mass loss rate (mg/min), A_0 is the Knudsen cell orifice area (cm^2), and K is the equilibrium constant for the homogeneous equilibrium between S(g) and S_2(g). The relation between K and temperature was obtained from Mills' compilation.[23]

The mass-loss rates at each temperature, and the partial pressures of ytterbium, sulfur and S_2 obtained, are listed in Tables 2.2 - 2.4. The LnP_i vs 1/T for individual partial

pressures are plotted in Figure 2.2. A linear least squares fit to all the data for each species yielded:

$$\mathrm{LnP_S(atm)} = -\frac{53932(\pm 679)}{T} + 14.93(\pm 0.39) \qquad (2.5)$$

$$\mathrm{LnP_{S_2}(atm)} = -\frac{55091 \pm 1357}{T} + 15.30(\pm 0.77) \qquad (2.6)$$

$$\mathrm{LnP_{Yb}(atm)} = -\frac{54521 \pm 1028}{T} + 16.70(\pm 0.58) \qquad (2.7)$$

The second- and third-law enthalpies and entropies of the reaction (2.1) were obtained by plotting $-(\mathrm{RLnK} + \Delta\mathrm{fef_T})$ vs 1/T to obtain the slope and by a point-by-point evaluation of $-\mathrm{T}(\mathrm{RLnK} + \Delta\mathrm{fef_T})$, respectively. The free energy functions for S(g) and S_2(g) were obtained from the JANAF tables,[24] and for Yb(g) from Hultgren.[25] The free energy function for $Yb_{0.877}S$(s) was obtained from the following estimation: by use of the Kubaschewski approximation,[26] the heat capacity of $Yb_{0.877}S$ is approximated to be $Cp = 10.585 + 1.4944\times10^{-3}T$. Errors of ±1 kcal $mole^{-1}$ in the enthalpy functions and ±1 cal $mole^{-1}$ K^{-1} in the entropy and the free energy functions were assumed to result from the Cp described above. The standard entropy of $Yb_{0.877}S$(s) was

Table 2.2. First run data and results
Orifice area = $1.29 \times 10^{-2} cm^2$

T (K)	$\Delta m/\Delta t \times 10^3$ (mg/min)	$P_S \times 10^7$ (atm)	$P_{S_2} \times 10^7$ (atm)	$P_{Yb} \times 10^7$ (atm)	ΔH°_{298} (kcal/mole)
1762	6.92	1.36	0.896	5.35	203.2
1811	16.9	3.26	2.29	13.2	202.7
1664	1.46	0.263	0.195	1.10	202.2
1736	5.23	0.972	0.707	4.02	202.4
1786	12.1	2.27	1.67	9.42	202.3
1711	3.18	0.598	0.418	2.42	202.7
1797	14.6	2.74	2.02	11.4	202.4
1748	5.76	1.11	0.754	4.44	202.9
1827	24.4	4.56	3.44	19.2	202.1
1724	3.92	0.743	0.515	3.00	202.7
1840	29.3	5.51	4.14	23.2	202.2
1688	2.03	0.383	0.262	1.54	202.8
1760	8.38	1.53	1.16	6.48	202.1
1774	9.85	1.85	1.34	7.64	202.4

Table 2 3. Second Run data and results
Orifice area: $1.29 \times 10^{-2} cm^2$

T (K)	$\Delta m/\Delta t \times 10^3$ (mg/min)	$P_S \times 10^7$ (atm)	$P_{S_2} \times 10^7$ (atm)	$P_{Yb} \times 10^7$ (atm)	ΔH°_{298} (kcal/mole)
1712	3.22	0.607	0.423	2.45	202.3
1762	7.98	1.49	1.08	6.17	202.4
1787	12.2	2.29	1.68	9.50	202.4
1703	2.72	0.511	0.356	2.07	202.6
1736	5.48	1.00	0.752	4.21	202.1
1774	10.4	1.92	1.45	8.07	202.1
1723	4.35	0.791	0.595	3.33	202.5
1793	14.3	2.65	2.00	11.2	202.1
1751	6.47	1.22	0.868	4.99	202.6
1723	3.90	0.736	0.514	2.98	202.1
1810	18.5	3.45	2.60	14.5	202.2
1712	3.45	0.635	0.464	2.63	202.7
1820	20.6	3.93	2.84	16.2	202.5
1743	5.94	1.10	0.807	4.57	202.3

Table 2.3. (continued)

T (K)	$\Delta m/\Delta t \times 10^3$ (mg/min)	$P_S \times 10^7$ (atm)	$P_{S_2} \times 10^7$ (atm)	$P_{Yb} \times 10^7$ (atm)	ΔH°_{298} (kcal/mole)
1832	24.3	4.67	3.35	19.2	202.6
1760	6.17	1.25	0.771	4.77	203.7
1801	14.9	2.84	2.03	11.6	202.6
1693	2.39	0.441	0.17	1.81	202.4
1741	5.63	1.05	0.759	4.33	202.4

Table 2.4. Third run data and results
Orifice area: $8.81 \times 10^{-3} cm^2$

T (K)	$\Delta m/\Delta t \times 10^3$ (mg/min)	$P_S \times 10^7$ (atm)	$P_{S_2} \times 10^7$ (atm)	$P_{Yb} \times 10^7$ (atm)	ΔH°_{298} (kcal/mole)
1713	2.92	0.736	0.612	3.26	201.3
1773	7.82	2.03	1.65	8.89	201.5
1733	3.90	1.00	0.809	4.38	201.6
1813	14.4	3.82	3.04	16.5	201.7
1753	5.26	1.39	1.08	5.94	201.8
1791	10.5	2.76	2.24	11.9	201.6
1723	3.30	0.848	0.683	3.70	201.5
1832	21.4	5.52	4.68	24.7	201.2
1783	9.05	2.37	1.91	10.3	201.6
1695	1.80	0.476	0.357	2.00	202.1
1802	13.2	3.39	2.85	15.1	201.2
1743	4.38	1.16	0.893	4.94	201.9
1762	6.50	1.69	1.36	7.36	201.6

Table 2.4.(Continued)

T (K)	$\Delta m/\Delta t \times 10^3$ (mg/min)	$P_S \times 10^7$ (atm)	$P_{S_2} \times 10^7$ (atm)	$P_{Yb} \times 10^7$ (atm)	ΔH°_{298} (kcal/mole)
1703	2.57	0.632	0.546	2.86	201.0
1821	17.8	4.61	3.86	20.5	201.3
1841	23.4	6.14	5.06	27.1	201.4

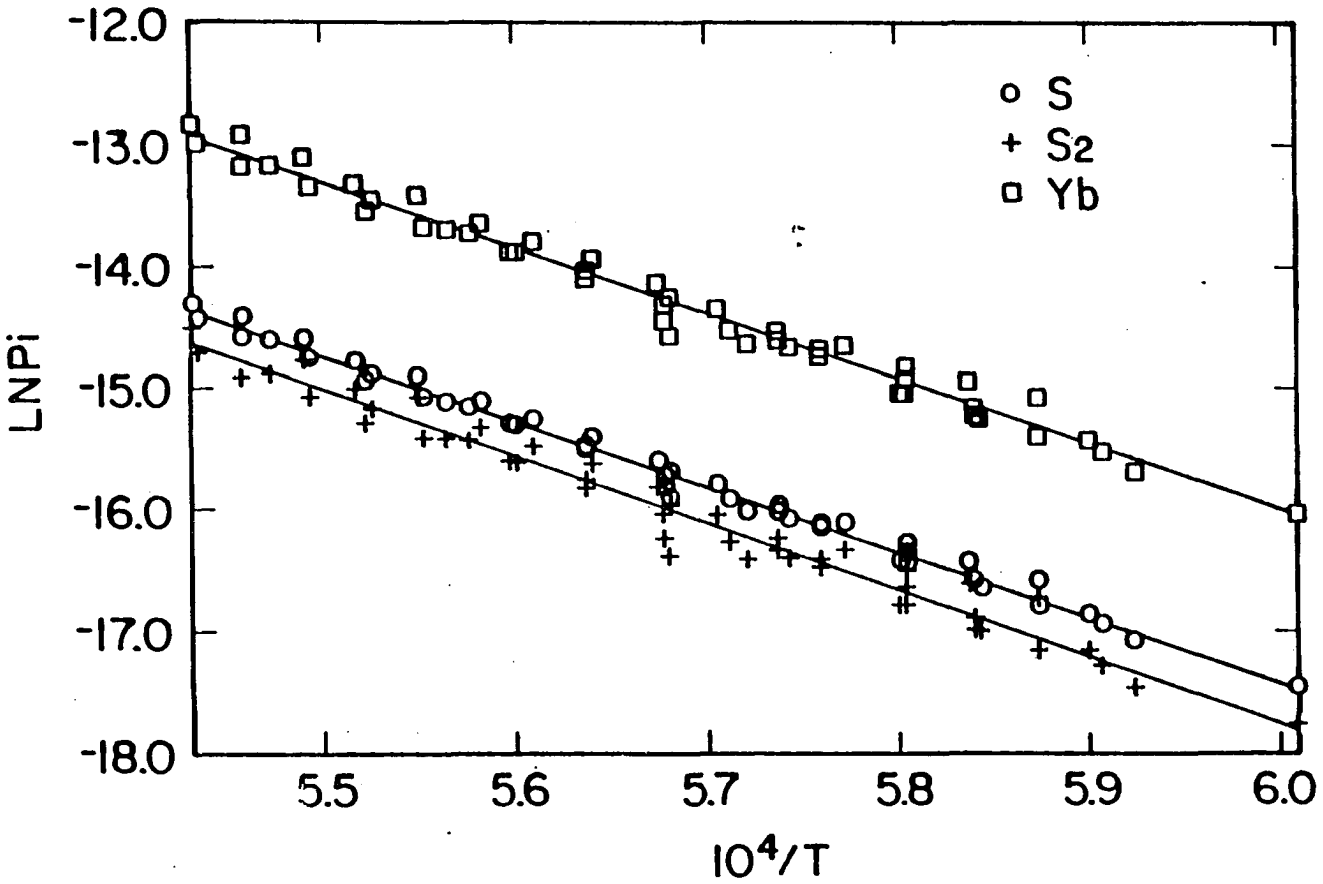

Figure 2.2 LnP_{Yb}, LnP_S and LnP_{YbS} vs $10^4/T$ (Pressure in atm)

estimated to be 15.9(±1.0) cal $mole^{-1}$ K^{-1} by comparing with the standard entropies of YbS(s) and Yb_2S_3(s).[23] The configurational contribution of the random ytterbium vacancies was also included.

From all the data the following results were obtained: the second-law enthalpy and entropy change for reaction (2.1) are: ΔH°_{298} = 204.0(±5.0) kcal $mole^{-1}$, ΔS°_{298} = 61.7(±3.0) cal $mole^{-1}$ K^{-1}. The third-law results are: ΔH°_{298} = 202.2(±2.0) kcal $mole^{-1}$ and ΔS°_{298} = 60.5(±1.0) cal $mole^{-1}$ K^{-1} (Table 2.5)

Table 2.5. Second- and third-law results

Third-law		Second-law	
ΔH°_{298} (kcal/mole)	[a]ΔS°_{298} (cal/mole K)	ΔH°_{298} (kcal/mole)	ΔH°_{298} (cal/mole K)
202.2(2.0)	60.5(1.0)	204.0(5.0)	61.7(3.0)

[a]Calculated from reference data.

DISCUSSION

In this work, we found that $Yb_{0.877}S$ undergoes a first order phase transition at about 1373K. The low temperature form has a NaCl-type superstructure, while the high temperature form has simple NaCl-type structure with a random distribution of ytterbium vacancies. Since the thermodynamic measurement was undertaken at temperatures above the order-disorder transition temperature, the $Yb_{0.877}S(s)$ samples for which the mass-loss rate were measured have the simple NaCl-type structure with randomly distributed ytterbium vacancies. Thus the thermodynamic results deduced at 298K in the result section are based on the congruent vaporization reaction: $Yb_{0.877}S$ (s, NaCl-type structure) = 0.877Yb(g) + S(g) (2.8). At room temperature, however, stable $Yb_{0.877}S(s)$ has a NaCl-type superstructure. The entropy change during the change from ordered structure to disordered structure can be estimated to be the configurational contribution of the random ytterbium vacancies, which is 0.741 cal $mole^{-1}$ K^{-1}. The enthalpy change during the first order phase transition is then estimated to be: $\Delta H_{tr} = T_{tr}\Delta S_{tr}$ = 1 kcal $mole^{-1}$ K^{-1}. Accordingly, for the dissociation reaction $Yb_{0.877}S$ (s, superstructure) = 0.877 Yb(g) + S(g), the second-law thermodynamic results are: ΔH°_{298} = 205.0(±5.0) kcal $mole^{-1}$, ΔS°_{298}

= 62.4(±3.0) cal mole^{-1} K^{-1}; The third-law result is: ΔH°_{298} = 203.2(±2.0) kcal mole^{-1}.

The mode of vaporization of $Yb_{0.877}S$ is different from that reported for other congruently vaporizing lanthanide sulfides, except europium monosulfide. The monosulfide gaseous species are significant during the congruent vaporization of LaS,[27,28] PrS,[29] Pr_3S_4,[29] GdS,[30] Lu_3S_4[31] and $Sc_{0.8065}S$.[32,33] $Yb_{0.877}S$, however, similar to EuS, vaporizes entirely as the atomic species. The congruent vaporization of $Yb_{0.877}S$ reflects some characteristics similar to those observed in the Sc-S system where $Sc_{0.8065}S$ vaporizes congruently. Both congruently vaporizing solids have the NaCl-type structure with metal vacancies. Tuenge et al[32] estimated the enthalpy change for the reaction ScS(s) = $Sc_{0.8065}S$(s) + 0.1935 Sc(g) to be 17.5±2 kcal mole^{-1} by using scandium partial pressure data. During our vaporization behavior study, it was found that ytterbium monosulfide loses ytterbium at partial pressures of metal that are greater than in the case of ScS(s) at comparable temperatures. It is concluded that the enthalpy change for reaction YbS(s) = $Yb_{0.877}S$(s) + 0.123Yb(g) (2.9) is less than 17.5 kcal mole^{-1}. The atomization energy of stoichiometric YbS(s) can be obtained by combining reaction (2.1) and (2.9). The ΔH°_{298} is then within the range 204 - 221 kcal mole^{-1}. These

values are correlate well with the dissociation energy of EuS(s),[34] which is 215.4±1.2 kcal $mole^{-1}$.

Fenochka and Gordienko[21] found the dissociation energy of YbS(s) at 298K to be 199.4±2.0 kcal mol^{-1} by mass spectrometric measurement over the temperature range 1670 - 2030 K. According to our experience, YbS(s) loses Yb very quickly over the above temperature range, and the composition changes to a congruent composition. Therefore, the measured vapor species are in equilibrium with $Yb_{1-x}S(s)$ rather than YbS(s), as assumed in their study.

REFERENCES

1. Villars, P.; Calvert, L. D. Pearson's Handbook of Crystallographic Data for Intermetallic Phases; American Society of Metals: Metals Park, Ohio, 1985.

2. Kuz'micheva, G. M.; Borodulenko, G. P.; Grizik. A. A.; Eliseev, A. A. Russ. J. Inorg. Chem., 1975, 20(3), 465.

3. Patrie, M. Bull. Soc. Chim. France, 1969, 5, 1600.

4. Eliseev, A. A.; Kuz'micheva, G. M.; Pisarev, E.A.; Borodulenko, G. P.; Grizik, A. A. Russ. J. Inorg. Chem., 1975, 20(5), 657.

5. Kuz'micheva, G. M.; Eliseev, A. A. Russ. J. Inorg. Chem., 1977, 22(4), 497.

6. Eliseev, A. A.; Kuz'micheva, G. M.; Yashnov,V. I. Russ. J. Inorg. Chem., 1978, 23(2), 273.

7. Kuz'micheva, G. M.; Efremov, V. A.; Khlyustova, S. Y.; Eliseev, A. A. Russ. J. Inorg. Chem., 1986, 31(9), 1273.

8. Drafall, L. E.; Mccarthy, G. J.; Sipe, C. A.; White, W. B. Proceedings of the Rare Earth Research Conf., 1974, 11th. 2, 954

9. Iandelli, A.; Palenzona, A. Proprietes Thermodynamiques Physiques et Structurales des Derives Semi-metalliques, Colloques Internationaux du Centre National de la Recherche Scientifique, Orsay, 1965, p. 397

10. Sleight, A. W.; Prewitt, C. T. Inorg. Chem., 1968, 7, 2282

11. Flahaut, J.; Domange, L.; Pardo, M. C. R. Acad. Sci. Paris, 1964, 258, 594

12. Range, K. J.; Leeb, R. Zeitschrift fuer Naturforschung, Teil B: Anog. Chemie, Organische Chemie, 1975, 30, 889

13. Eatough, N. L.; Webb, A. W.; Hall, H. T. Inorg. Chem., 1969, 8, 2069

14. Lashkarev, G. V.; Radzikovskaya, S. V.; Radchenko, M. V. Inorg. Mat.(Eng. Tran.), 1971, 7, 767

15. Flahaut, J.; Domage,L.; Loriers, J. C. R. Acad. Sci. Ser.C, 1958, 247, 1614.

16. Francillon, M.; Jerome, D.; Achard, J. C.; Malfait, G. J. de Physique, 1970, 31, 709.

17. Flahaut, J.; Domange, L.; Guittard, M.; Loriers, J. Bull. Soc. Chim. France, 1961, 1, 102.

18. Tomas, A.; Robert, M.; Guittard, M. Mat. Res. Bull., 1988, 23, 507.

19. Otero-diaz, L. C.; Landa-canovas, A. R.; Hyde, B. G. J. Solid State Chem., 1990, 89, 237.

20. Chevalier, R.; Laruelle, P.; Flahaut, J. Bull. Soc. fr. Mineral. Crystallogr., 1967, 564.

21. Fenochka, B. V.; Gordienko, S. P. Russ. J. Phys. Chem., 1973, 47(9), 1384.

22. Smoes, S.; Coppens, P.; Bergman, C.; Drowart, J. Tran. Faraday Soc., 1969, 65, 682.

23. Mills, K. C. Thermodynamic data for Inorg. Sulphides, Selenides and Tellurides; Butterworths: London, 1974.

24. Chase, M. W. Jr.; Davies, C. A.; Downey, J. R.; Frurip, D. J.; McDonald, R. A.; Syverud, A. N. JANAF Thermodynamic Tables; American Chemical Society and the American Institute of Physics for the National Bureau of Standards: Midland, 3rd ed.; 1986; 1779.

25. Hultgren, R.; Desai, P. D.; Hawkins, D. T.; Gleiser, M.; Kelley, K. K.; Wagman, D. D.Selected Values of the Thermodynamic Properties of the Elements; American Society for Metals: Metals Park, OH, 1973; p 344.

26. Kubaschewski, O. Metallurgical Thermochemistry; Pergamon: New York, 5th ed.; 1979; p 183.

27. Cater, E. D.; Lee, T. E.; Johnson, E. W.; Rauh, E. G.; Eick, H. A. J. Phys. Chem., 1965, 69, 2684.

28. Cater, E. D.; Steiger, R. P.J. Phys. Chem., 1968, 70, 2231.

29. Cater, E. D.; Barbara, H. M.; Fries, J. A. NBS Spec. Publ., 1979, 561, 237.

30. Fries, J. A.; Cater, E. D. J. Chem. Phys., 1978, 68, 3978.

31. Franzen, H. F.; Hariharan, A. V. J. Chem. Phys., 1979, 70, 4907.

32. Tuenge, R. T.; Laabs, F.; Franzen, H. F. J. Chem. Phys., 1976, 65, 2400.

33. Nakahara, J. F.; Franzen, H. F. High Temp. Sci., 1986, 22, 195.

34. Hariharan, A. V.; Eick, H. A. High Temp. Sci., 1971, 3, 123.

SECTION III. TWO NEW THULIUM SULFIDES

REVIEW OF PREVIOUS WORK

The binary thulium sulfides found previously between 0 and 60% atomic percent sulfur are: TmS, Tm_2S_3 and Tm_5S_7. Their structure data are summarized in Table 3.1. Tm_2S_3 has six different structural types depending on temperature and pressure.[1] At a preparation temperature of about 1000°C, Tm_2S_3 occurs in the monoclinic δ-form.[2] The cubic θ-phase of Tm_2S_3 with space group $Ia\bar{3}$ was first obtained by Patrie[3] from the elements at 800°C. The given cell parameter of a = 10.51Å was questioned by Range et al.[1] They thought the wrong number was given perhaps due to a misprint and they gave the value of a = 12.51Å by analogy with Tl_2O_3-type Yb_2S_3. Kuz'micheva et al.[4] confirmed that a equals 12.51Å in their single crystal work. They also reported defects on the sulfur position. Their thermal stability study on θ-Tm_2S_3 in the temperature range 720 - 850°C showed that the compound loses sulfur as the temperature is increased, resulting in an increase of the sulfur vacancies and a decrease in the lattice parameter. Eliseev and coworkers[5] suggested that the ε-Tm_2S_3 has space group P6/mmm, while Range et al.[6] found that ε-Tm_2S_3 crystallizes in a rhombohedral structure of corundum-type with the same cell parameters obtained by Eliseev et al. The three other Tm_2S_3 phases with structure

types: $CeYb_3S_6$,[7] U_2S_3[8] and Th_3P_4[1] were obtained at high temperature and high pressure.

Thulium monosulfide has the NaCl type structure. The cell parameter was determined to be 5.412Å by Flahaut et al.,[9] Guittard[10] and Iandelli.[11] Bucher et al.[12] and Clayman et al.[13] reported values of 5.420Å and 5.45Å, respectively. No homogeneity study was performed on TmS.

A series of $Ce_4Lu_{11}S_{22}$[14] type ternary $L_4Tm_{11}S_{22}$ (L = La, Ce, Pr, Nd, Sm) compounds was obtained by Vovan and coworkers.[15] In this type of compounds the light rare earths (La, Ce, Pr, Nd, Sm) always have coordination numbers of seven or eight, while thulium always has coordination numbers of six and seven. The only observed binary rare earth chalcogenide with this type of structure was $Yb_{15}S_{22}$, which exists at high temperature and high pressure, and was written as $YbS.7Yb_2S_3$ by Range.[16] This phase was found to coexist with $CeYb_3S_6$-type, Ho_2S_3-type Yb_2S_3, Yb_5S_7 or defect Yb_3S_4. No structural data for this phase was reported.

Chouteau and coworkers[17] showed the relationship between magnetic susceptibility and temperature of TmS (Figure 3.1) in comparision with TmSe. TmS obeys the Curie Weiss Law between the Néel temperature (T_N ~ 7 K) and room temperature. Bucher et al.[12] obtained the effective moment of TmS to be 7.19 μ_B, which indicates a slight reduction compared with the theoretical value

Table 3.1. Crystallographic data for Tm-S system

PHASE	STRUCTURE TYPE	SPACE GROUP	LATTICE PARAMETERS				REFERENCE
			a(Å)	b(Å)	c(Å)	BETA(DEG.)	
TmS	NaCl	$Fm\bar{3}m$	5.412				9, 10, 11
Tm_5S_7	Y_5S_7	C2/m	12.628	3.761	11.462	104.82	18
$Tm_2S_3(\delta)$	Ho_2S_3	$P2_1/m$	10.037	3.954	17.350	98.68	2
Tm_2S_3	Th_3P_4	$I\bar{4}3d$	8.223				1
$Tm_2S_3(\varepsilon)$	Corundum	$R\bar{3}c$	6.768		18.236		6
$Tm_2S_3(\theta)$	Tl_2O_3	$Ia\bar{3}$	10.51				3
Tm_2S_3	CeYb3S6	$P2_1/m$	10.870	3.873	11.104	108.92	7
Tm_2S_3	U_2S_3	Pnma	10.479	3.803	10.360		8

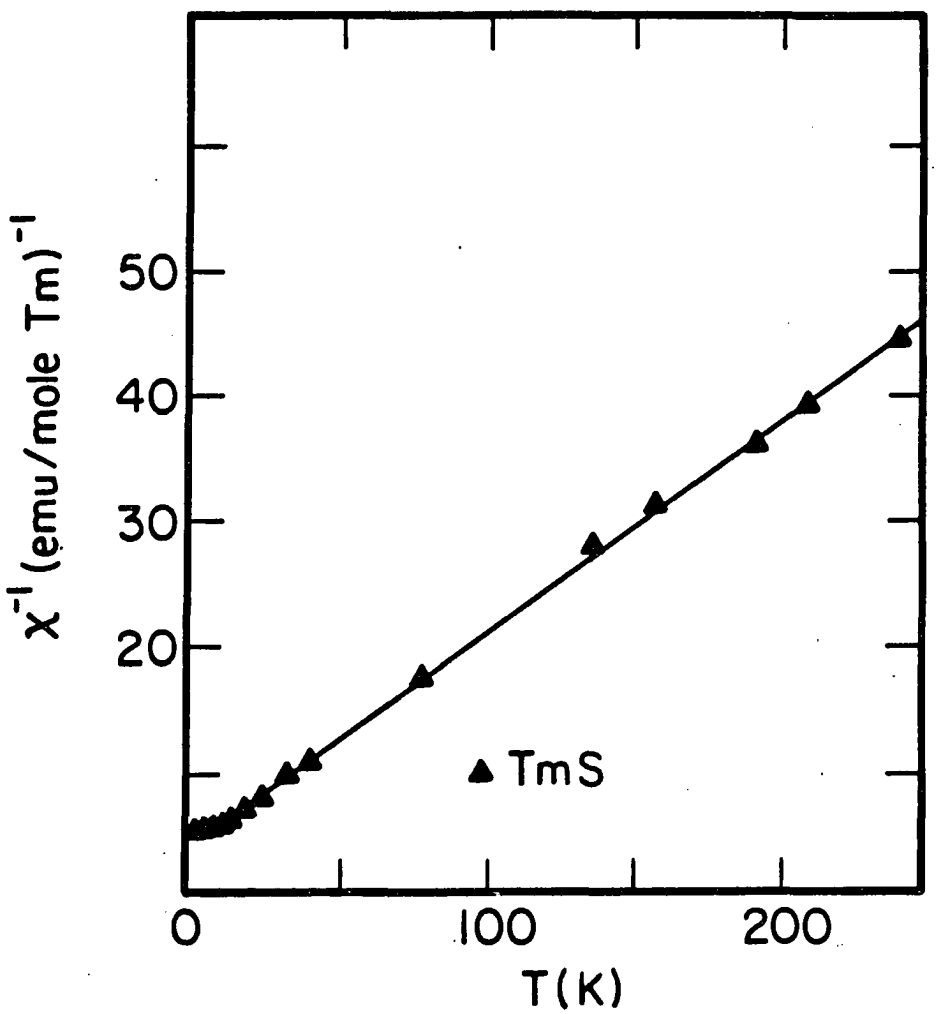

Figure 3.1 Temperature dependence of the magnetic susceptibility of TmS

of 7.56 μ_B. They thought that the crystal-splitting or slight sulfur excess may partially account for the discrepancy. X-ray photoelectron spectra done by Campagna et al.[19] showed the trivalent character of Tm in TmS, and Batlogg[20] confirmed the Tm valence state of +3 in TmS by optical measurement. TmS exhibits antiferromagnetic order at low temperature. Koehler and Moon[21] obtained the Néel temperature T_N ~ 8.9 K from neutron diffraction studies on powder and single crystal TmS between 1.7 K and room temperature, while Flouquet and coworkers[22] reported T_N ~ 5.2 K. This value agrees well with that obtained by other methods. Flouquet's results also showed that the magnetic structure of TmS is of the same type as that of $CeAl_2$ at low temperature. Berger et al.[23] measured the electrical resistivity of TmS in the temperature range of 20 mK to 300 K. They found that with decreasing temperature the resistivities increase gradually in general agreement with the results reported by Bucher and coworkers.[12] Between ~10 and 300 K, the resistivities have a logarithmic temperature dependence (Figure 3.2). A resistivity maximum observed at about 10 K is attributed to the Kondo resistivity of TmS and the Néel temperature is about 6 K.

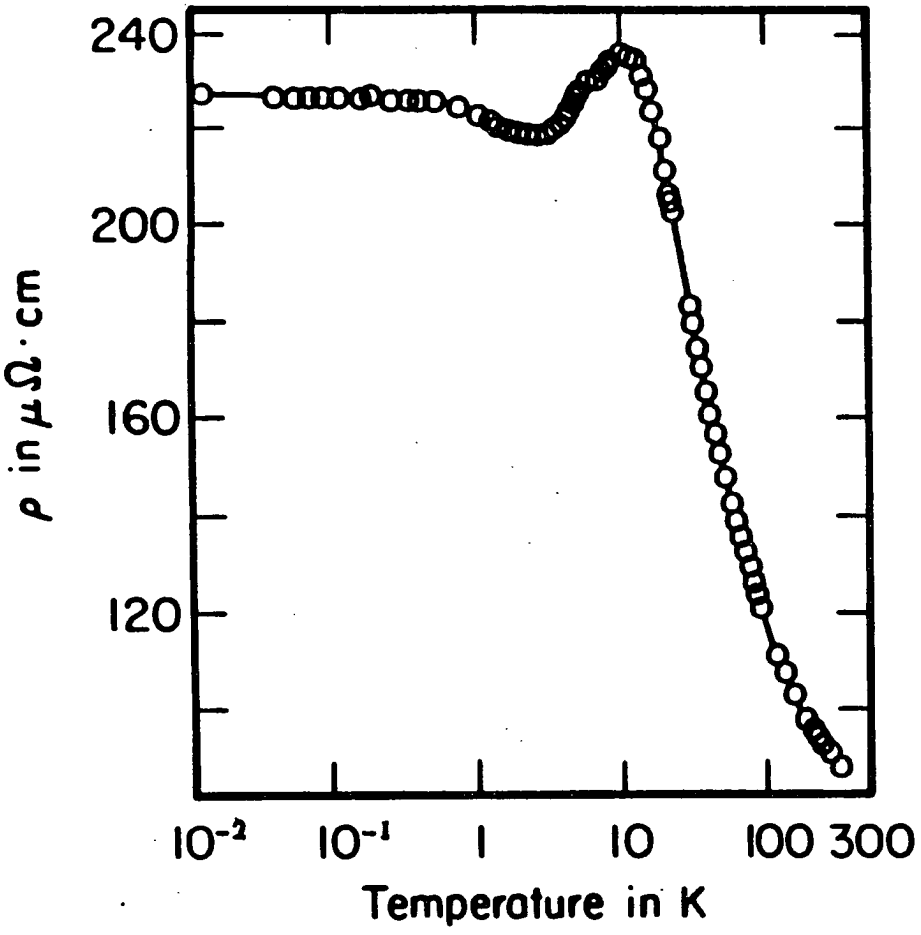

(a)

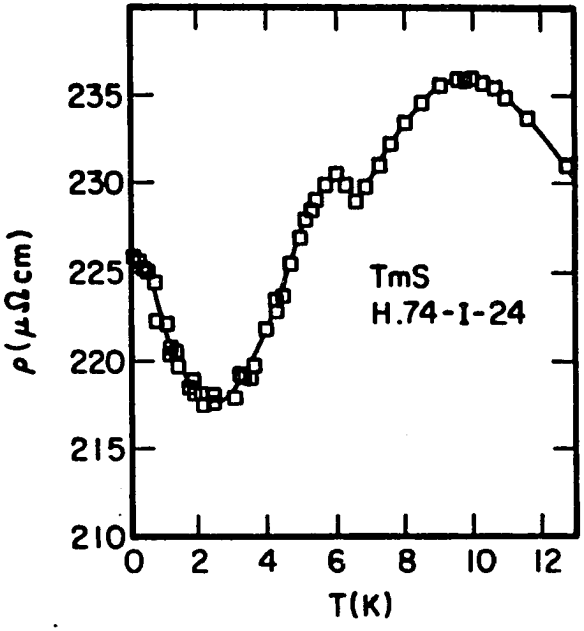

(b)

Figure 3.2 (a) Resistivity vs LogT of TmS.
(b) Resistivity vs T of TmS at low temperature

Bucher et al.[12] also reported that δ-Tm_2S_3 with the Ho_2S_3-type structure, θ-Tm_2S_3 with the Tl_2O_3-type structure and Tm_5S_7 are all probably Van Vleck paramagnets. No ordering could be detected down to 0.5K for δ- and θ-Tm_2S_3, while the black metallic Tm_5S_7 showed antiferromagnetic order near 0.6 K.

SAMPLE PREPARATION AND PHASE ANALYSIS

Samples with compositions in the range S/Tm = 0.9 - 1.5 were prepared in the manner described in the experimental section. It was found that below 600°C no obvious reaction between thulium metal and sulfur was observed. Thus temperatures of the tube furnace were raised above this temperature over several hours to enhance the reaction rate. The homogenized samples obtained from high temperature inductive heating were analyzed by Guinier powder diffraction. The phases observed were: TmS, Tm_5S_7 and Tm_2S_3. Only two polymorphic structures of Tm_2S_3 were observed, i.e., Tm_2S_3 with the Ho_2S_3-type structure (δ-Tm_2S_3) and Tm_2S_3 with the corundum-type structure (ε-Tm_2S_3). δ-Tm_2S_3 was obtained below 1300°C, while ε-Tm_2S_3 was found in samples quenched from above this temperature. θ-Tm_2S_3 was not observed in this study. The powder pattern of ε-Tm_2S_3 was indexed and the cell parameters obtained are: a = b = 6.7768(5)Å, c = 18.239(2)Å, β = 120°, which agree with what was found by Range et al.[6] and Eliseev.[5] A transparent single crystal was obtained from the melts. The space group was determined to be $R\bar{3}c$, which confirms the space group obtained by Range.[6]

When a sample with composition S/Tm = 1.0 was inductively heated at high temperature in a tungsten crucible with a small

orifice, it vaporized incongruently and the composition changed toward the sulfur richer side. When the S/Tm ratio reached about 1.20, a new phase was observed with weak lines on the Guinier powder pattern and the lines became stronger and stronger as the sample continuing to vaporize. The composition of this new phase was later determined to be Tm_8S_{11} by single crystal x-ray diffraction. It was found that Tm_8S_{11} vaporized incongruently towards Tm_5S_7, which vaporized congruently. The vaporization rate of Tm_8S_{11} was found to be fairly low below 1350°C and the composition changed a little when it was heated below this temperature.

Indications of the existence of a new phase between Tm_5S_7 and Tm_2S_3 were first found on a Guinier powder diffraction pattern of the incongruent vaporization product of Tm_2S_3 (Ho_2S_3-type). The vaporization temperature was about 1800K. Further study showed that this phase appears in the quenched products only when the sample is melted, and it disproportionates into the neighboring phases when the melted sample is annealed at about 1200°C. The composition of this new phase was determined to be $Tm_{15}S_{22}$ by single crystal x-ray diffraction.

Vaporization and thermodynamic studies on congrently vaporizing compound Tm_5S_7 were performed and no meaningful

results could be obtained because of the low volatility of Tm_5S_7 even up to its melting point.

PART I. SYNTHESIS, CRYSTAL STRUCTURE AND MAGNETIC PROPERTIES OF Tm_8S_{11}

EXPERIMENTAL DETAILS

Single Crystal Growth

An "x-ray pure" sample of Tm_8S_{11} was prepared in three steps: first, a stoichiometric mixture of thulium and sulfur was heated in an evacuated quartz glass ampoule at 700°C for two weeks. The prepared sample was then homogenized, placed in a tungsten crucible and inductively heated up to ~1320°C for two days. Subsequently, the homogeneous, black-colored material was annealed in a sealed quartz glass tube at 750°C for one week and finally cooled down to room temperature within three days. A plate-like single crystal was picked from the final sample.

Magnetic Susceptibility Measurements

The magnetometric measurements were carried on a 47.15 mg sample of Tm_8S_{11} in the temperature range 1.56 - 259.3 K by means of Faraday magnetometor under a field of 0.656 T.

RESULTS AND DISCUSSION

Structure Determination

The stucture was solved in collaboration with Dr. Harbrecht at Universität Dortmund of Germany by single crystal x-ray diffraction.

The translational and rotational symmetry was determined from a plate-like crystal(0.12mm x 0.17mm x 0.06mm) employing a Buerger precession camera (zirconium-filtered Mo Kα radiation). The integral and zonal extinctions were in accord with the centrosymmetric space group Cmcm and two polar subgroups thereof ($Cmc2_1$ and Ama2). All 54 reflections ($0° \leq 2\theta \leq 68°$) of a Guinier powder pattern ($\lambda(Cu\ K\alpha_1)$ = 1.5051Å) could be indexed without contradiction to Cmcm symmetry. The least-squares refinements led to a = 3.7486(4), b = 12.6160(8), c = 34.932(3)Å.

X-ray intensity data in the range $1° < \phi < 35°$ were collected on a CAD 4B diffractometer (Enraf Nonius, Delft) with Mo Kα radiation (Graphite monochromator in incident beam, λ = 0.71073Å).

Reflections with $-6 \leq h \leq 6$, $0 \leq k \leq 20$ and $0 \leq l \leq 56$ were monitored in the ω-2θ mode (scan width: $1.0 + 0.35 \tan \phi$). Three orientation and intensity control reflections were measured each

150 reflections and 10,000 s respectively. No reorientation and loss of intensity was observed. The transmission factors derived from azimuthal scans of five reflections ranged from 0.557 to 0.998. Merging of 3794 reflections led to 2059 reflections with R(I) = 0.097. Structure calculations were performed with the program package SDP (Enraf Nonius, version 3.1, 1988). Scattering factors including the corrections for anomalous dispersion were taken from the International Tables of Crystallography.

The thulium partial structure was solved by direct methods in the space group Cmcm. In order to refine the positional and thermal parameters, least-squares calculations were performed minimizing $w|F_0^2 - F_c^2|^2$ with w based on counting statistics $\sigma(I)$ ($w = 4F_0^2/\sigma^2(F_0^2)$; $\sigma^2(F_0^2) = \sigma^2(I) + 0.003F_0^2$). The positions of the sulfur atoms were obtained from diffrence Fourier calculations. Before the data were averaged and the coefficients of the anisotropic temperature factors were refined, a numerical absorption correction,[24] with correction factors ranging from 0.765 to 1.292, was applied to the data. For all five crystallographic distinct thulium atoms a refinement of the multiplicity revealed that deviations from full occupancy are less than 1.8%. The final refinements (61 variables) were done with 883 unique reflections in the range $0.10 \leq \sin\theta/\lambda \leq 0.75$

with $I \geq 3\sigma(I)$. The residual charge density scaled to ρ_{max} (S) is 0.072, R(I) = 0.067, $R_w(I)$ = 0.088, S = 1.075. Crystal data for Tm_8S_{11} are listed in Table 3.1. Positional and equivalent isotropic B values are listed in Table 3.2. The interatomic distances are reported in Table 3.3.

Structural Features

Tm_8S_{11} is the first rare earth chalcogenide with 8:11 stoichiometry. It can be rationalized as a 3:2 compound in the Tm_2S_3-TmS section of the binary system. The coordination polyhedra for the crystallographically distinct thulium atoms are distorted octahedra for Tm1 (2.636, 2.693, <2.66>), Tm4 (2.635-2.772, <2.680>), Tm5 (2.648-2.729, <2.69>), a distorted trigonal prism for Tm2 (2.690, 2.830, <2.780>) and a capped trigonal prism for Tm3 (2.708-2.881, <2.80>). The number in parentheses corresponds to the range and mean values of Tm-S bonding distances (in Å), sulfur atoms are four- and five-fold coordinated: S1 <2.66> and S2 <2.67> are in distorted tetrahedra, S6 <2.65> is in rectangle, S3 <2.76>, S4 <2.76> and S5 <2.80> are in distorted square pyramid.

Table 3.2. Crystal data for Tm_8S_{11}

Space group	Cmcm		
Z	4		
Lattice parameters			
a(Å)	3.7486(4)[a]		3.743(1)[b]
b(Å)	12.6160(8)		12.602(3)
c(Å)	34.932(3)		34.917(8)
Volume(Å^3)	1652.0		1647.0
Density (g cm^{-3})	6.851		
Unique reflections($I \geq 3\sigma(I)$)	883		
Variables	61		
R(I); R(F)	0.067; 0.043		

[a]Guinier

[b]Diffractometer.

Table 3.3. Positional and thermal parameters for Tm_8S_{11}

Atom	Wrckoff notation	Point symmetry	x	y	z	$^aB_{eq}$
Tm1	4a	2/m	0	0	0	0.42(2)
Tm2	4c	mm	0	0.5070(1)	0.25	1.02(3)
Tm3	8f	m	0	0.25787(6)	0.05876(3)	0.47(1)
Tm4	8f	m	0	0.2416696)	0.68297(3)	0.44(2)
Tm5	8f	m	0	0.01927(6)	0.13307(3)	0.35(1)
S1	4c	mm	0	0.8541(6)	0.25	0.6(1)
S2	8f	m	0	0.0894(4)	0.5682(2)	0.60(9)
S3	8f	m	0	0.1142(4)	0.2967(2)	0.48(8)
S4	8f	m	0	0.3532(3)	0.5159(2)	0.46(9)
S5	8f	m	0	0.3363(4)	0.6113(2)	0.51(9)
S6	8f	m	0	0.3942(4)	0.3377(2)	1.0(1)

$$^aB_{eq} = 4/3 \left(a^2B_{11} + b^2B_{22} + c^2B_{33} \right)$$

Table 3.4. Interatomic Distance(in Å)

Tm(1)-S(2)	4x2.636(6)	Tm(2)-S(1)	2x2.690(65
S(4)	2x2.693(3)	S(3)	4x2.830(4)
Tm(3)-S(2)	2x2.708(4)	Tm(4)-S(1)	2.635(3)
S(4)	2x2.778(4)	S(6)	2x2.641(4)
	2.872(6)	S(3)	2x2.706(4)
S(5)	2x2.881(5)	S(5)	2.772(6)
Tm(5)-S(2)	2.648(6)		
S(6)	2x2.654(4)	Tm ... Tm > 3.725(1)	
S(5)	2x2.722(4)	S ... S > 3.265(9)	
S(3)	2.729(6)		
Ave. Tm - S	2.725		

All motifs of coordination in Tm_8S_{11} are also present in monoclinic Tm_5S_7 (a = 12.628, b = 3.761, c = 11.462Å, β = 104.82°).[18,25] The similarity between the two structures is already reflected in the lengths of the a and b axes. A projection of the structure of Tm_8S_{11} along the a axis is depicted in Figure 3.3, which also shows the structural relationship to Tm_5S_7. The sequence of layers along the c axis, identified according to the nature of thulium coordinations, is opoopo (o, octahedral; p, trigonal prismatic) for Tm_5S_7 and opoopoopo for Tm_8S_{11}. Doubling of the sequence for the new sulfide is associated with inversion at z = 1/2 module c giving rise to a long c axis.

Owing to the lack of short distances for S-S (the shortest is 3.265Å) and Tm-Tm (the shortest is 3.722Å) the expected average oxidation state for thulium is +2.75. According to Shannon[26], the ionic radii for Tm^{+2} and Tm^{+3} ions are 1.03Å and 0.880Å respectively, for coordination number(CN) 6. The value for Tm^{+3}, CN 8 is 0.994Å, for S^{2-}, CN 6 is 1.84Å. Therefore, we are inclined to attribute valence +2 to Tm2 and, if the remaining 4f electrons are also localized, to 50% of Tm3. At this point it should be mentioned that the structure derived so far does not allow a complete ordering of Tm^{+2} and Tm^{+3} ions. The larger mean distance of Tm2-S and the exceptional high temperature factor B_{eq} = 1.02$Å^2$ of Tm2 (definitely not caused by defects, because the

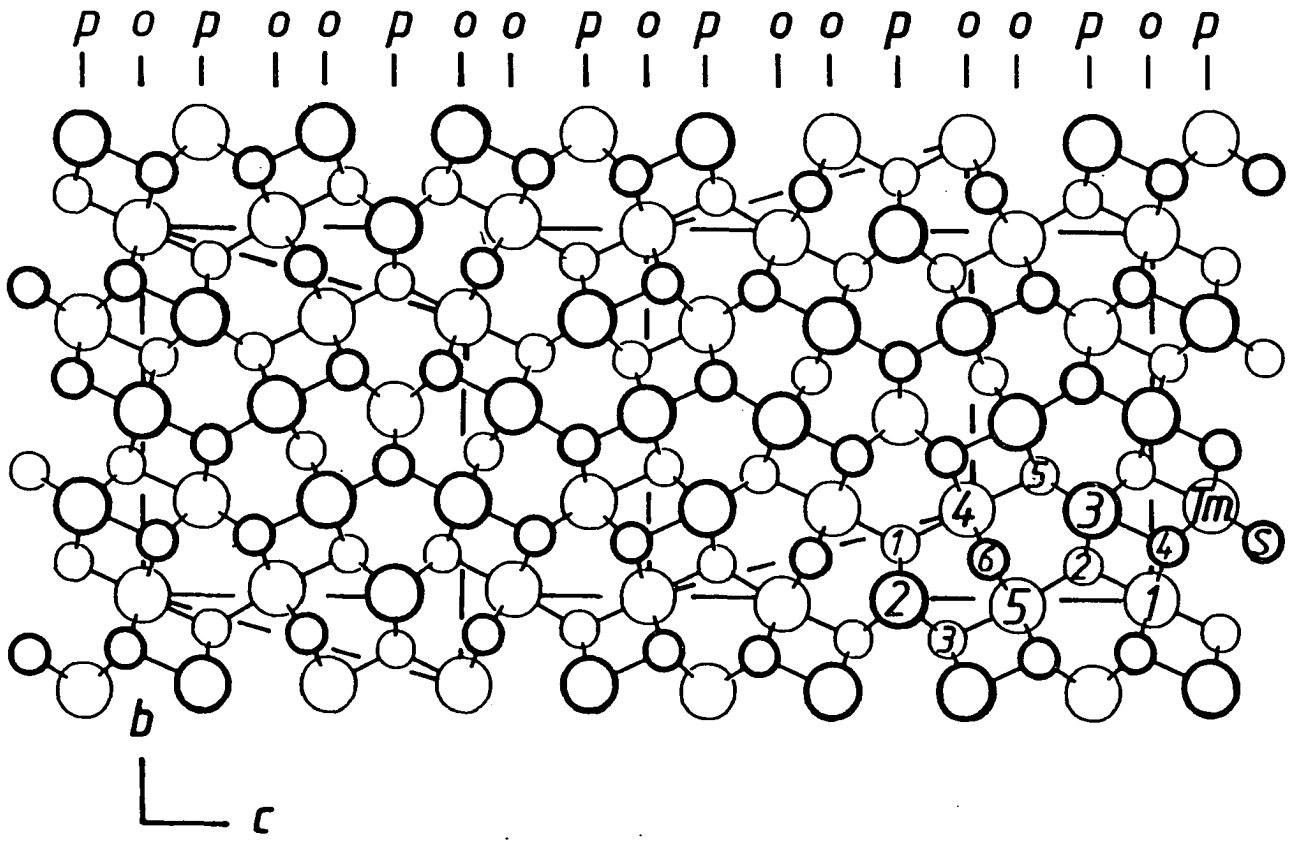

Figure 3.3 Projection of the structure of Tm_8S_{11} along a; traces of two unit cells of the structure of Tm_5S_7 (ac projections) are also shown

population factor f=0.993(5) if refined) may be indicative of a matrix effect rather than of valence +2 for Tm2.

Magnetic Susceptibilities

Additional information about the electronic state of thulium in Tm_8S_{11} is gained from magnetic susceptibilities χ. The temperature dependence of χ points to a magnetic ordering below 7 K (Figure 3.4). Above the presumed Néel temperature, it basically obeys the Curie-Wiess Law (Figure 3.5).

The effective paramagnetic moment μ_{eff} deduced from χ^{-1} vs T in the temperature range 150 - 259 K is 7.50 μ_B, which is in a good agreement with theoretical value 7.56 μ_B, the theoretical value for free Tm^{3+} ions. According to these findings all thulium atoms in Tm_8S_{11} have oxidation state of +3 and eight electrons per cell are delocalized. Thus Tm_8S_{11} is expected to be a metallic conductor. It proved to be a conductor when the resistance of a pressed pellet was measured using a multimeter.

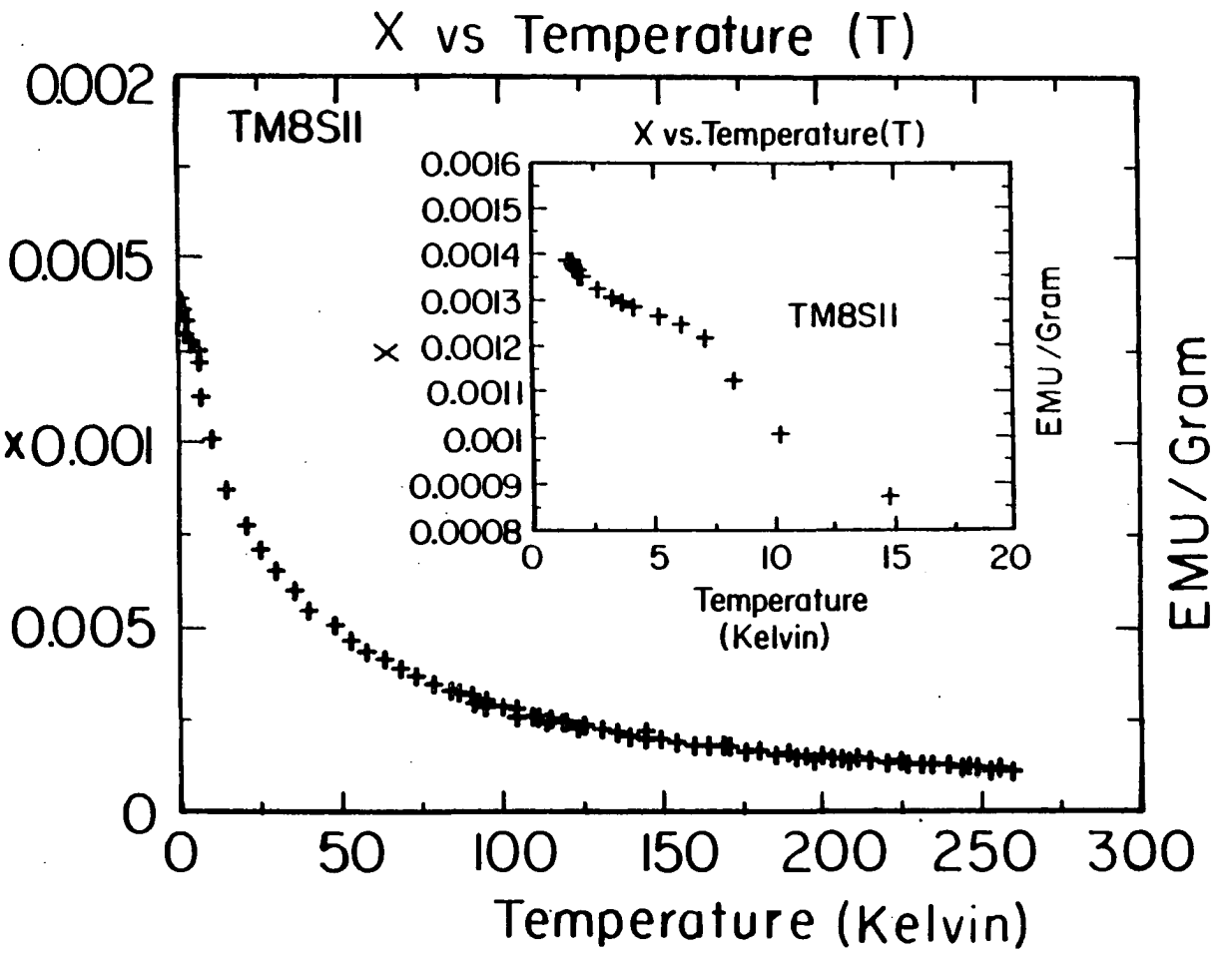

Figure 3.4 Temperature dependence of magnetic susceptibility of Tm_8S_{11}

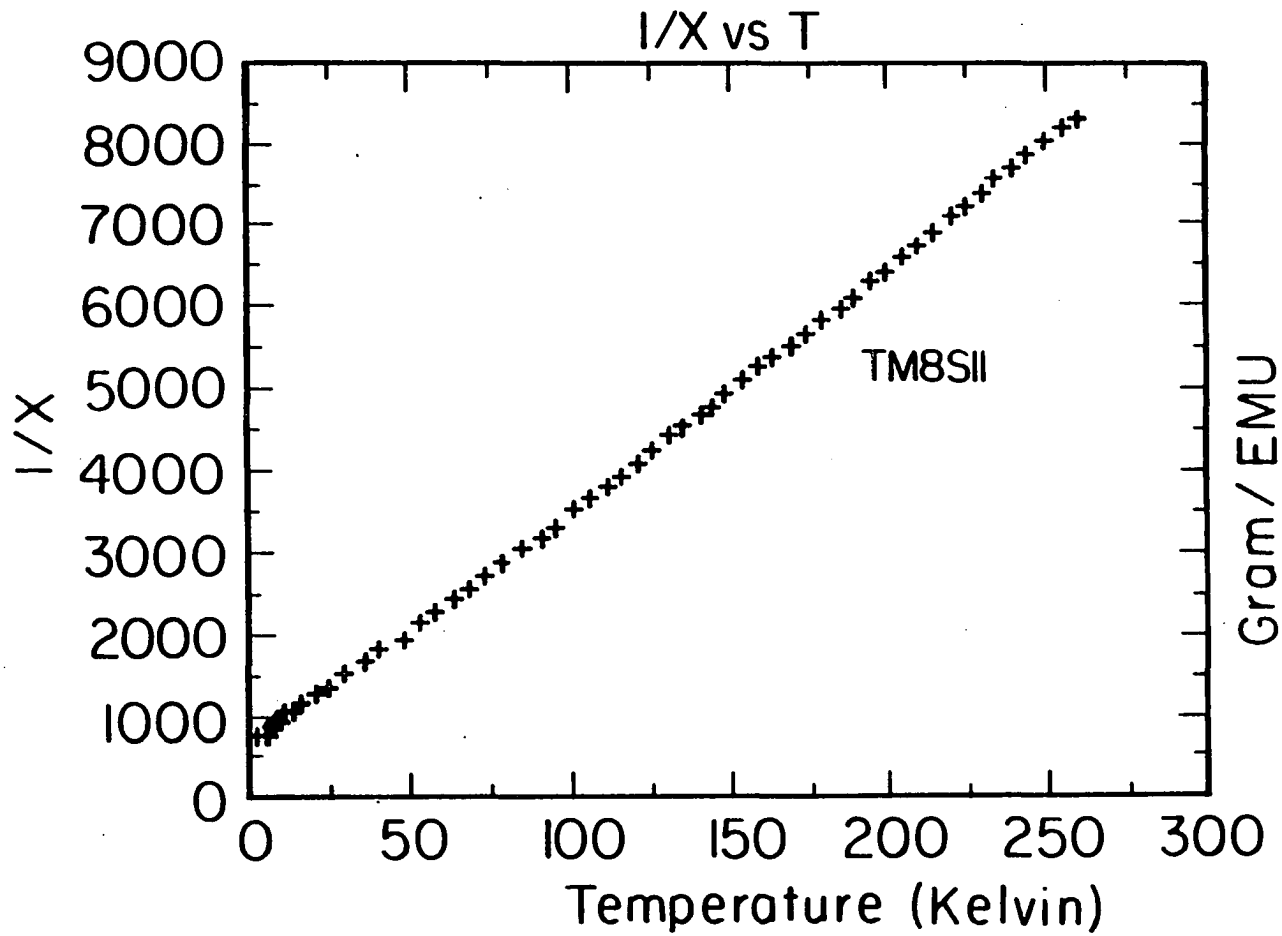

Figure 3.5 Inverse magnetic susceptibility of Tm_8S_{11} vs temperature

PART II. SINGLE CRYSTAL DETERMINATION OF $Tm_{15}S_{22}$

EXPERIMENTAL DETAILS

Single Crystal Growth

The thulium sulfides with composition in the range $1.4 \leq S/Tm \leq 1.5$ were vaporized, melted and quenched to room temperature. The residual samples were always a mixture of Tm_5S_7 and $Tm_{15}S_{22}$, or of $Tm_{15}S_{22}$ and Tm_2S_3. A black colored, plate shaped single crystal used in the x-ray study was picked from the mixture of $Tm_{15}S_{22}$ and Tm_5S_7 which resulted from the continuous vaporization and melting of the initial compound Tm_5S_7. The mixture contains about 70% $Tm_{15}S_{22}$. Several crystals of $Tm_{15}S_{22}$ picked from this mixture were examined by energy-dispersive analysis by x-rays (EDAX) in a scanning electron microscope. The results showed that only thulium and sulfur are present in the sample. Attempts to synthesize single phase $Tm_{15}S_{22}$ were unsuccessful.

Crystallography

The possible space groups of $Tm_{15}S_{22}$ were determined to be a centrosymmetric space group C2/m and two noncentrosymmetric space

groups C2, Cm on the basis of observed extinction conditions on the Weissenberg, rotation photographs and the Laue check on a RIGAKU AFC6R single-crystal diffractometer.

Intensity data from the $Tm_{15}S_{22}$ single crystal were collected on a RIGAKU AFC6R single crystal diffractometer with monochromatic Mo Kα radiation, the ω-scan technique was employed up to 50° (2θ). From the total 3359 reflections ($\pm$h, k, $\pm$l), 1072 independent reflections with $I > 3\sigma_I$ were obtained and used for the structure analysis. An absorption correction was applied. No decay correction was applied since no remarkable decay was observed on the standard reflections during the data collection. Other important crystal and refinement data are listed in Table 3.5.

The structure was determined using the program TEXSAN. The Tm partial structure was solved by the direct method (SHELX-86) in the space group C2/m. The positions of the S atoms were obtained from difference Fourier calculations. The positional and thermal parameters were refined by standard least-squares full-matrix calculations. Before the anisotropic temperature factors were refined, the F_0 values were corrected for absorption effects with the program DIFABS[24] in the mode that utilizes θ-dependent systematic deviations $|F_0| - |F_c|$, the transmission coefficient ranged from 0.893 to 1.08. No fractional occupancy

was observed for the Tm positions. The positional and thermal parameters are listed in Table 3.6 and the interatomic distances are reported in Table 3.7. Powder pattern of $Tm_{15}S_{22}$ taken on a Guinier camera was indexed using the structural model obtained in this single crystal work and all the lines were successfully indexed.

Table 3.5. Crystal Data for $Tm_{15}S_{22}$

Space group	$C_{2/m}$(No 12)	
Z	2	
Lattice parameters:		
a,Å	38.31(1)[a]	38.395(4)[b]
b,Å	3.8343(7)[a]	3.8421(5)[b]
c,Å	11.103(4)[a]	11.141(2)[b]
β,degree	90.92(3)[a]	91.02(1)[b]
V,Å^3	1630.8(9)[a]	1643.2(4)[b]
D_{calcd}	6.596	6.546
Instrument	RIGAKU AFC6R	
Radiation	Mo Kα (λ=0.71079Å)	
	Graphite-monochromated	
μ(MoKα)	421.35	
Temperature	23°C	
$2\theta_{max}$	50.00°	
Scan mode	ω scan	
No. indep. obs.($I>3\sigma_I$)	1072	
No. variables	114	
R[c]	2.56	
R_w[c]	2.95	
Max. shift in final cycle	0.02	
Goodness of fit	1.04	
Max. peak in final. diff. map	2.91e$^-$/Å^3	
Second extinction coeff.	2.26×10^{-8}	

[a]Diffractometer
[b]Guinier

[c] $R = \sum_{i=1}^{n} (|F_{obs}|_i - |F_{calc}|_i) / \sum_{i=1}^{n} |F_{obs}|_i$;

$R_w = \sum_{i=1}^{n} [w_i (|F_{obs}|_i - |F_{calc}|_i)^2 / \sum_{i=1}^{n} w_i |F_{obs}|^2]^{1/2}$, $w_i = 1/\sigma^2(F_{obs})_i$

Table 3.6. Positional and thermal parameters for $Tm_{15}S_{22}$

Atom	x	y	z	$B_{(eq)}$[a]	U_{11}[b]	U_{22}[b]	U_{33}[b]	U_{12}[b]	U_{13}[b]	U_{23}[b]
Tm(1)	0.13330(3)	0	0.6572(1)	0.88(4)	0.0152(5)	0.0086(6)	0.0097(6)	0	0.0035(4)	0
Tm(2)	0.06861(3)	0.5	0.3582(1)	0.74(4)	0.0107(5)	0.0088(6)	0.0086(6)	0	-0.0022(4)	0
Tm(3)	0.03929(3)	0	-0.2740(1)	0.82(5)	0.0111(5)	0.0089(6)	0.0110(6)	0	-0.0003(4)	0
Tm(4)	0.29879(3)	0	0.05681(1)	0.64(4)	0.0096(5)	0.0085(6)	0.0062(5)	0	0.0009(4)	0
Tm(5)	0.5	0	0	0.92(7)	0.0090(7)	0.012(1)	0.0144(8)	0	0.0024(6)	0
Tm(6)	0.76545(3)	0	0.3529(1)	0.70(4)	0.0100(5)	0.0084(6)	0.0083(5)	0	0.0011(4)	0
Tm(7)	0.15718(3)	0	0.3054(1)	0.62(4)	0.0078(5)	0.0090(6)	0.0068(5)	0	-0.0014(4)	0
Tm(8)	0.39524(3)	0	0.9894(1)	0.71(4)	0.0069(5)	0.0098(6)	0.0103(5)	0	0.0002(4)	0
S(1)	0.0489(2)	0	0.9679(5)	0.5(2)	0.006(2)	0.006(3)	0.009(3)	0	0.001(2)	0
S(2)	0.2201(1)	0	0.4084(5)	0.7(2)	0.005(3)	0.012(4)	0.011(3)	0	-0.000(2)	0
S(3)	0.1470(1)	0	0.9078(5)	0.7(2)	0.008(3)	0.014(4)	0.005(3)	0	0.002(2)	0
S(4)	0.9928(1)	0.5	0.7616(6)	0.9(2)	0.003(3)	0.007(3)	0.023(3)	0	0.000(2)	0
S(5)	0.1668(1)	0.5	0.1494(5)	0.8(2)	0.011(3)	0.015(4)	0.006(3)	0	-0.001(2)	0

Table 3.6. (Continued)

Atom	x	y	z	$B_{(eq)}$[a]	U_{11}[b]	U_{22}[b]	U_{33}[b]	U_{12}[b]	U_{13}[b]	U_{23}[b]
S(6)	0.2449(2)	0	0.8799(5)	0.9(2)	0.013(3)	0.016(4)	0.006(3)	0	-0.001(2)	0
S(7)	0.0900(1)	0.5	0.7514(5)	0.6(2)	0.006(3)	0.005(3)	0.011(3)	0	-0.001(2)	0
S(8)	0.0930(1)	0	0.2061(5)	0.7(2)	0.010(3)	0.012(4)	0.004(3)	0	-0.003(2)	0
S(9)	0.3138(1)	0	0.3078(5)	0.5(2)	0.010(3)	0.006(3)	0.005(3)	0	-0.003(2)	0
S(10)	0.6340(1)	0	0.4618(5)	0.9(3)	0.012(3)	0.013(4)	0.007(3)	0	-0.000(2)	0
S(11)	0.0527(3)	0	0.5030(7)	4.5(5)	0.14(1)	0.014(5)	0.023(4)	0	0.053(6)	0

[a] $B_{eq} = (8\pi^2/3) \sum_{i=1}^{3} \sum_{i=1}^{3} U_{ij} a_i^* a_j^* a_i a_j$

[b] The form of the anisotropic displacement parameter is:

$$\exp[-2\pi^2 (a^{*2}U_{11}h^2 + b^{*2}U_{22}k^2 + c^{*2}U_{33}l^2 + 2a^*b^*U_{12}hk + 2a^*c^*U_{13}hl + 2b^*c^*U_{23}kl)$$

Table 3.7. Interatomic Distance (in Å)

Tm(1)-S(3)	2.832(6)	Tm(2)-S(4)	2.688(6)	Tm(3)-S(1)	2.714(6)
S(7)	2x2.759(4)	S(8)	2x2.738(4)	S(4)	2x2.657(4)
S(9)	2x2.817(4)	S(10)	2.744(6)	S(7)	4x2.748(4)
S(10)	2x2.904(5)	S(11)	2x2.589(5)	S(11)	2.546(7)
Tm(4)-S(3)	2x2.855(4)	Tm(5)-S(1)	4x2.715(4)	Tm(6)-S(2)	2x2.674(4)
S(5)	2.670(6)	S(4)	2x2.666(6)		2.707(6)
S(6)	2x2.653(4)			S(6)	2.617(6)
	2.833(6)			S(9)	2x2.726(4)
S(9)	2.846(6)				
Tm(7)-S(2)	2.654(6)	Tm(8)-S(1)	2x2.912(5)		
S(5)	2x2.622(4)	S(3)	2x2.774(4)	S ... S >	3.122(8)
S(8)	2.684(6)	S(5)	2.816(6)	Tm ... Tm >	3.7
S(10)	2x2.752(4)	S(7)	2.933(6)	Ave. Tm - S	2.75
		S(8)	2x2.945(4)		

RESULTS AND DISCUSSION

$Tm_{15}S_{22}$, like Tm_8S_{11}, is a rare-earth sulfide with unusual stoichiometry and a large cell. It can be rationalized as a 5:1 compound in the Tm_2S_3-Tm_5S_7 section of the binary system. Figure 3.6 represents the structure of $Tm_{15}S_{22}$ projected along b axis. The structure type of $Tm_{15}S_{22}$ is isostructural with $Ce_4Lu_{11}S_{22}$. No eight coordination polyhedra exists for Tm atoms in $Ce_4Lu_{11}S_{22}$ type $L_4Tm_{11}S_{22}$ (L=La, Ce, Pr, Nd, Sm) compounds, while it exists in $Tm_{15}S_{22}$. The close relationship between the structures of $Ce_4Lu_{11}S_{22}$ and $CeYb_3S_6$[27] was discussed by Rodier et al.[14] Since $CeYb_3S_6$ is isostructural with Tm_2S_3[7] (space group $P2_1/m$, a = 10.872, b = 3.874, c = 11.104Å, β = 108.92°), the structural relation between $Tm_{15}S_{22}$ and Tm_2S_3 is the same as that between $Ce_4Lu_{11}S_{22}$ and $CeYb_3S_6$. The coordination polyhedra in this compound are similar to those found in other rare-earth chalcogenides.[28] The coordination polyhedra of Tm2, Tm3, Tm5, Tm6, Tm7 are distorted octahedra, of Tm4 is capped distorted octahedron, of Tm1 is a capped trigonal prism and of Tm8 is a bicapped trigonal prism. The longest bonding distance of Tm - S is that between Tm8 and S8. The sulfur atoms are five or four coordinated: S1, S3, S7, S8, S9, S10 have distorted square pyramidal coordination, S2, S4, S5, S6 have distorted tetrahedral

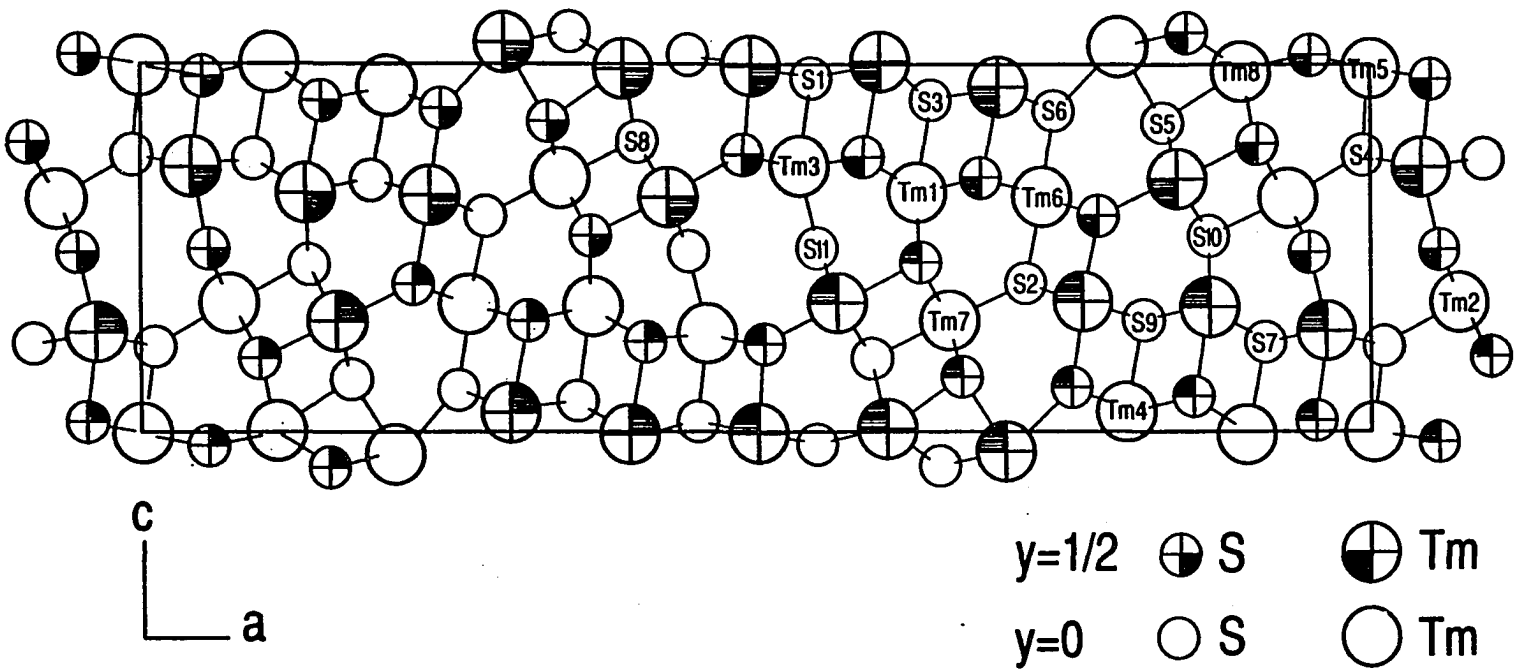

Figure 3.6 Projection of the structure of $Tm_{15}S_{22}$ along b axis

coordination and S11 has a distorted trigonal planar coordination. The three-fold coordination of S11 is unusual. The fourth nearest Tm atom (Tm1) is 3.51Å distant from S11 and the average nearest neighbor bonding distance for Tm-S in this structure is 2.75Å. The unusual high thermal parameter (B_{eq} = 4.5Å^2) and the elongated anisotropic thermal ellipsoid (U_{11}:U_{22}:U_{33} = 10:1:1.6) of S11 reflect its unsymmetrical environment. There are two holes adjacent to S11 along the a direction, which is the principal direction of elongation of the thermal ellipsoid of S11. A similar elongation was observed in the structure of $K_2Tm_{23.33}S_{36}$.[29] In this structure there is a channel along the c axis with maximum diameter at the origin of the unit cell. The S atom next to it has a very high thermal parameter (B_{eq} = 6.59Å^2). Attempts to refine the structure of $Tm_{15}S_{22}$ in the noncentrosymmetric space group Cm failed, while reduction to the space group C2 yielded a solution similar to that reported. Attempts to move S11 off the refined position or to split S11 onto two separate positions with half occupancy failed. No additional reflections suggesting an ordered superstructure of $Tm_{15}S_{22}$ were observed on either Wiessenberg, rotation photographs or the powder pattern taken on a Guinier camera. Thus we are left with the conclusion that the S11 position is either disordered in some unspecified, spatial

distribution or the unsymmetric environment of S11 causes unusually anisotropic thermal motion.

REFERENCES

1. Range, K. J.; Gietl, A.; Klement, U.; Lange, K. G. J. Less-Common Metals, 1990, 158, L21.

2. Sleight, A. W.; Prewitt, C. T. Inorg. Chem., 1968, 7, 2282.

3. Patrie, M. Bull. Soc. Chim. France, 1969, 1600.

4. Kuz'micheva, G. M.; Smarina, E. I.; Khlyustova, S. Y.; Chernyshev, V. V. Russ. J. Inorg. Chem., 1990, 35(4), 488.

5. Eliseev, A. A.; Grizik, A. A.; Kuz'micheva, G. M.; Borodulenko, G. P. Russ. J. Inorg. Chem., 1975, 20(7), 973.

6. Range, K. J.; Drexler, H.; Gietl, A.; Klement, U.; Lange, K. G. Acta Cryst., 1990, C46, 487.

7. Range, K. J.; Leeb, R. Z. Naturforsch.Teil B., 1976, 31, 311.

8. Range, K. J.; Leeb, R. Z. Naturforsch.Teil B., 1975, 30, 889.

9. Flahaut, J.; Guittard, M.; Gorochov, O.; Wintenberger Colloq. Intern. Centre Natl. Rech. Sci. Paris, 1967, 157, 431.

10. Guittaid, M. Compt. Rend., 1965, 261, 2109.

11. Iandelli, A. Rare Earth Res. Semin., Lake Arrowhead, Calif., 1960, P.135.

12. Bucher, E.; Andres, A.; di Salvo, F. J. Phys. Rev., 1975, B11, 500.

13. Clayman, B. P.; Ward, R. W.; Tidman, J. P. Phys. Rev., 1977, B16, 3734.

14. Rodier, N.; Vovan, T. Bull Soc. Fr. Mineral. Crystallogr., 1975, 98, 30.

15. Vovan, T.; Guittard, M.; Rodier, N. Mat. Res. Bull., 1979, 14, 597.

16. Range, K. J.; Lange, K. G.; Drexler, H. Comments Inorg. Chem., 1984, 3, 171.

17. Chouteau, G.; Holtzberg, F.; Pena, O.; Penney, T.; Tournier, R. J. de. Physique, Colloque C5, Supp. 5, Vol. 39, 1979, C5-361.

18. Adolphe, C. Compt. Rend., 1964, 258, 4773

19. Campagna, M.; Wertheim, G. K.; Bucher, E. Struc. Bonding [Berlin], 1976, 30, 119.

20. Batlogg, B. Phys. Rev., 1981, B23, 1827.

21. Koehler, W. C.; Moon, R. M. J. Appl. Phys., 1979, 50(3), 1975.

22. Flouquet, J.; Haen, P.; Vettier, C. J. Magn. Magn. Mater., 1982, 29, 159.

23. Berger, A.; Bucher, E.; Haen, P.; Holtzberg, F.; Lapierre, F.; Penney, T.; Tournier, R. Valence Instab. Relat. Narrow-Band Phenomen. Proc. Intern. Conf.; Rochester: N.Y., 1976(1977); P 491.

24. Walker, N.; Stuart, D. Acta Crystallog. Sec. A, 1983, 39, 158.

25. Adophe, C. Ann. Chim., 1965, 10, 271.

26. Shannon, R. D. Acta Crystallogr. Sec. A, 1976, 32, 751.

27. Rodier, N.; Vovan, T. C. R. Acad. Sci., 1974, 279, 817

28. Gschneidner, K. A. Jr.; Eyring, L. Handbook on the Phys. and Chem. of Rare Earths; North-Holland: Amsterdam, 1979; Chap. 31; p 5.

29. Lemoine, P.; Tomas, A.; Carre, D.; Vovan, T.; Guittard, M. Acta Crystallogr. Ser., 1989, C45, 350.

GENERAL SUMMARY

High temperature vaporization and thermodynamic studies showed that the congruently vaporizing compounds found in both Nd-S and Yb-S systems are nonstoichiometric compounds, which are $NdS_{1.38}(s)$ and $Yb_{0.877}S(s)$. The congruent vaporization reactions of $NdS_{1.38}(s)$ are: $NdS_{1.38}(s) = NdS(g) + 0.38\ S(g)$ (I) and $NdS_{1.38}(s) = Nd(g) + S(g)$ (II), of $Yb_{0.877}S(S)$ is: $Yb_{0.877}(s) = 0.877\ Yb(g) + S(g)$ (III). The atomization or cohesive energies of these two compounds were found to be 302.3±2.0 kcal $mole^{-1}$ and 203.2±2.0 kcal $mole^{-1}$ respectively, which are the enthalpy changes of reactions (II) and (III). By analogy with $Sc_{0.8065}S(s)$, the atomization energy of YbS(s) is estimated within the range of 204 - 221 kcal $mole^{-1}$.

Tm_8S_{11} has a orthorhombic structure with space group Cmcm, cell parameters a = 3.7486(4), b = 12.6160(8), c = 34.932(3)Å. It is a new structure type for rare earth chalcogenides and the stoichiometry has not been reported previously. All Tm atoms in this compound are trivalent and it was found to be a metallic conductor due to the existence of free electrons in this compound. $Tm_{15}S_{22}$ is isostructural with $L_4Tm_{11}S_{22}$ (L = La, Ce, Pr, Nd, Sm) with space group C2/m, a = 38.395(4), b = 3.8421(5), c = 11.141(2)Å, β = 91.01°. The eight coordination polyhedra of

Tm exist in $Tm_{15}S_{22}$, while no coordination numbers of Tm larger than seven exist in $L_4Tm_{11}S_{22}$. In a small composition range from S/Tm = 1.375 to 1.50, four compounds: Tm_8S_{11}, Tm_5S_7, $Tm_{15}S_{22}$ and Tm_2S_3 exist and their stoichiometries are very close and the structures of Tm_8S_{11} and Tm_5S_7, $Tm_{15}S_{22}$ and Tm_2S_3 are closely related to each other. As the composition changes from one compound to another, the structure does not change completely. As a matter of fact, part of the structure of one compound is retained in the structure of the adjacent compound. This observation makes us wonder what new phases with new stoichiometry but structure related to the known phases might exist in this narrow composition range and could be discovered by careful studies, such as the Kundsen effusion technique which proved to be so powerful and time-saving in our study.

ADDITIONAL REFERENCES

1. Samsonov, G. V. High-Temperature Compounds of Rare Earth Metals with Nonmetals; Consultants Bureau: New York, 1965; Chap. V.

2. Ho, J. C.; Taher, S. M. A.; King, G. B.; Gruber, J. B.; Beaudry, B. J.; K. A. Gschneidner, Jr. J. De Physique Colloque C6, Supp. 8, Vol. 39, 1978, C6-840.

3. Golubkov, A. V.; Sergeeva, V. M. Zhurnal Vses. Khim. Ob-va im. Mendeleeva, 1981, 26(6), 45.

4. Franzen, H. F.; Merrick, J. A. J. Solid State Chem. 1980, 33, 371.

5. Franzen, H. F.; Tuenge, R. T.; Eyring, L. J. Solid State Chem. 1983, 49, 206.

6. Tomas, A.; Robert, M.; Guittard, M. Mater. Res. Bull., 1988, 23, 507.

7. Hariharan, A. V.; Eick, H. A. High Temp. Sci., 1971, 3(2), 123

8. Cater, E. D.; Mueller, B. H.; Fries, J. A. NBS special publication 561, 1979, 237.

9. Bayanov, A. P. Russ. Chem. Rev., 1975, 44(2), 122.

10. Matignon, C. Ann. Chim. Phys., 1907, 10, 104.

11. Montgomery, R. L. U.S. Bur. Min., 1959, 5468.

12. Schiffman, R. A.; Franzen, H. F.; Ziegler, R. J. High Temp. Sci., 1982, 15, 69.

13. Kematick, R.; Anderegg, J.; Franzen, H. F. High Temp. Sci., 1985, 19(1), 17.

14. Knudsen, M. Ann. Physik, 1909, 28, 75.

15. Knudsen, M. Ann. Physik, 1909, 28, 999.

16. Dushman, S.; Lafferty, J. M. Scientific Foundations of Vacuum Technique; 2nd edition; John Wiley and Sons Inc.: New York, 1966.

ACKNOWLEGEMENTS

The author wishes to thank her major professor H. F. Franzen for his guidance, encouragement and enthusiasm throughout this work. Special thanks to Jim Anderegg, who helped the author from instrumentation to the equipment maintenance. The author also wish to express her gratitude to Dr. Ginke Tang who did the magnetic suscepitibity measurement and helped her to interpret the data. The friendship and helps from many friends and group members are also greatly appreciated.

The author is indebted to her parents, who raised her up through many difficult years and who always stand behind her.

The author wants to dedicate this dissertation to her husband, Qun Dou, to recognize his encouragement, support and inspiration throughout this work.

This work was performed at Ames Laboratory with the U.S. Department of Energy under Contract No. W-7405-Eng-82. This work was supported by the Office of Basic Energy Sciences, Materials Sciences Division.